DOE/MC/10637-3663
(DE94004080)

Low-Rank Coal Research

Annual Report (July 1, 1989 - June 30, 1990)
Including Quarterly Report (April - June 1990)

November 1990

Work Performed Under Contract No.: DE-FC21-86MC10637

For
U.S. Department of Energy
Office of Fossil Energy
Morgantown Energy Technology Center
Morgantown, West Virginia

By
University of North Dakota
Energy and Environmental Research Center
Grand Forks, North Dakota

DOE/MC/10637-3663
(DE94004080)
Distribution Category UC-105

Low-Rank Coal Research

Annual Report (July 1, 1989 - June 30, 1990)
Including Quarterly Report (April - June 1990)

Work Performed Under Contract No.: DE-FC21-86MC10637

For
U.S. Department of Energy
Office of Fossil Energy
Morgantown Energy Technology Center
P.O. Box 880
Morgantown, West Virginia 26507-0880

By
University of North Dakota
Energy and Environmental Research Center
Box 8213, University Station - UND
Grand Forks, North Dakota 58202

November 1990

TABLE OF CONTENTS

2.0 CONTROL TECHNOLOGY AND COAL PREPARATION RESEARCH

2.1 Flue Gas Cleanup

FLUE GAS CLEANUP

Annual Technical Project Report
for the Period July 1, 1989 through June 30, 1990

Including

the Quarterly Technical Progress Report
for the Period April 1 through June 30, 1990

by

Greg. F. Weber, Research Supervisor
Stan J. Miller, Senior Research Engineer
Dennis L. Laudal, Research Engineer

University of North Dakota
Energy & Environmental Research Center
Box 8213, University Station
Grand Forks, North Dakota 58202

Contracting Officer's Representative: Perry Bergman

for

United States Department of Energy
Pittsburgh Energy Technology Center
P.O. Box 10940 MS 922-H
Pittsburgh, Pennsylvania 15236

October 1990

Work Performed Under Cooperative Agreement No. DE-FC21-86MC10637

TABLE OF CONTENTS

LIST OF FIGURES

LIST OF FIGURES (Cont.)

LIST OF FIGURES (Cont.)

LIST OF TABLES

FLUE GAS CLEANUP

1.0 INTRODUCTION

In 1983 the Grand Forks Energy Technology Center of the U.S. Department of Energy was transferred to the University of North Dakota. From April 1, 1983, through June, 1987, the facility operated as a nonprofit contract research organization called the University of North Dakota Energy Research Center (UNDERC). In October 1989, the name was changed to the Energy and Environmental Research Center (EERC), University of North Dakota. Department of Energy programs ongoing at the time of the 1983 transfer were continued under a three-year Cooperative Agreement with the Department of Energy. In 1986 a second multiyear Cooperative Agreement (Contract No. DE-FC21-86MC10637) was signed by the Department of Energy.

From April 1983 through March 1988, the focus of the Cooperative Agreement SO_x/NO_x Control project was investigation of dry sorbent injection for SO_x control and methods of enhancing SO_x sorbent reactivity/utilization. The primary emphasis was furnace injection of calcium-based sorbents with some experiments evaluating backend humidification (1,2). In April 1988 the emphasis of the project was changed to advanced NO_x control with application to new and existing utility systems, as well as control of NO_x emissions from industrial-scale combustors. Specific activities for the period April 1988 through June 1989 focused on the bench-scale evaluation of a catalyst-coated woven fabric filter for simultaneous NO_x and particulate control (3).

In June 1989 the project name was changed from SO_x/NO_x Control to Flue Gas Cleanup, and the scope of project activities was expanded to include tasks supporting a bench-scale effort in fine particulate control. Work in the fine particulate control area was a separate project within the Cooperative Agreement from April 1983 through March 1988 and was also funded as a result of a competitive DOE award during the period May 1988 through December 1989.

This report documents the results for the Flue Gas Cleanup project for the period July 1, 1989, through June 30, 1990. The highlights of previous work, current program goals and objectives, fourth-year accomplishments on a task basis, and conclusions based on work completed are summarized.

2.0 BACKGROUND

2.1 Catalytic Fabric Filtration

Acid rain and the passage of legislation to reduce emissions of acid rain precursors continue to be prominent issues in the United States, Canada, Europe, and Japan. Although SO_2 emissions are still the primary focus of acid rain control legislation in the United States, the role of NO_x in acid rain formation and atmospheric ozone chemistry has resulted in NO_x emissions receiving prominent consideration in recent proposed legislation. In Europe, substantial reductions in NO_x emissions have been mandated, requiring local utilities to apply both staged combustion and post-combustion technologies to existing and new fossil fuel-fired systems.

Selective catalytic reduction (SCR) was developed by the Japanese to reduce NO_x emissions from oil- and gas-fired combustors. Conventional SCR technology involves applying a catalyst to a honeycomb type support structure which is located upstream of the air-heater. Ammonia is injected and thoroughly mixed with the flue gas upstream of the SCR reactor. As the flue gas passes through the SCR reactor, the catalyst provides sites where the NO_x and ammonia react to form nitrogen and water.

In response to restrictive NO_x regulations, SCR technology has been installed on 6,400 MW of full-scale utility boiler capacity in Europe (4), with a total of over 20,000 MW planned by the end of 1990. Application of conventional SCR technology to coal-fired systems presents several potential problems. The problems observed include plugging of the catalyst support structure by fly ash, deactivation of the catalyst by fly ash components and SO_3, deposition of sulfur and ammonia by-products on air-heater surfaces, and waste product handling/reuse/disposal.

Initial development of the catalyst-coated woven fabrics was funded exclusively by Owens-Corning Fiberglas Corp. (OCF). Following several years of in-house development, OCF contracted with the EERC to assist with the development effort. Due to funding constraints, the development work was discontinued in the fall of 1986. This initial work demonstrated the following with respect to the catalyst-coated fabric filter bag concept:

1. Good economic potential.

2. Over 90% reduction of NO_x in a flue gas stream.

3. Promising self-abrasion characteristics.

A more detailed summary of this earlier work was presented in the Final Technical Report for the period April 1, 1988, through June 30, 1989 (3).

In April of 1988 the development effort was resumed by OCF and the EERC. OCF activities were funded in-house and primarily involved preparation of catalyst-coated fabrics for bench-scale experiments performed at EERC. EERC's activities were funded within the DOE/EERC Cooperative Agreement and, to date, have focused on bench-scale experiments designed to show continuity with previous work and to screen samples of catalyst-coated fabric under both simulated (Task A) and actual flue gas conditions (Task B).

Task A was completed in May 1989, and the results are briefly summarized in the following discussion. A detailed summary of the results was presented in the Final Technical Report for the period April 1, 1988, through June 30, 1989 (3).

2.1.1 Parametric Evaluation

Following the construction and shakedown of the bench-scale experimental apparatus, two sets of parametric experiments (Task A.1 and A.3) were completed. This approach provided continuity with earlier work and helped evaluate specific operating conditions. Using a fabric similar to the fabric used during the original tests funded by OCF, experiments were conducted based on a full factorial design with four factors (air-to-cloth ratio, NO_x concentration, SO_2 concentration, and ammonia/NO_x molar ratio) and two levels (e.g.,

inlet NO_x concentrations of 300 ppm and 3000 ppm). After completing a statistical analysis of the data, the following conclusions were made:

1. The concentration of NO_x, the air-to-cloth ratio, and the interaction between these two parameters produce the greatest effect on NO_x removal. At a low air-to-cloth ratio (1.5 ft/min), an increase in NO_x concentration from 300 to 1000 ppm resulted in an increase in NO_x removal efficiency. When the air-to-cloth ratio was increased to 4 ft/min, an increase in NO_x concentration had no effect on NO_x removal efficiency. Increasing air-to-cloth ratio from 1.5 to 4.0 ft/min resulted in a decrease in the NO_x removal efficiency independent of NO_x concentration.

2. To a lesser degree, the ammonia/NO_x molar ratio, the SO_2 concentration, and the interaction between NO_x concentration and SO_2 concentration appeared to impact NO_x removal efficiency. As expected, increasing the ammonia/NO_x molar ratio from 0.8 to 1.1 increased the NO_x removal. But due to the limited range, the statistical significance of the effect was small. Although there was inconsistency in the data, increasing the SO_2 concentration from 300 to 3000 ppm decreased NO_x removal efficiency. Whether the effect was an artifact of the system is not known.

2.1.2 Fabric Screening Tests

Following the parametric evaluation, 16 fabrics were tested at constant conditions (Task A.2). These fabrics represented differences in catalyst composition and concentration, the use of different undercoatings, and the weave. The following conclusions were made as a result of the experimental series:

1. Addition of refractory components (Al or Zr) to the original V/Ti catalyst substantially reduced the reactivity of the catalyst-coated fabric.

2. The reactivity of the catalyst-coated fabric was improved by increasing the amount of catalyst on the fabric. Two approaches were tested with similar results. The first approach involved increasing the catalyst concentration in the coating solution, and the second approach involved coating a fabric sample several times using the same coating solution.

3. Application of a refractory undercoat prior to applying the catalyst coating did not appear to significantly impact the performance of the catalyst-coated fabric.

4. The use of a texturized cloth improved the performance of the catalyst-coated fabric in terms of higher NO_x removal efficiency and lower ammonia slip.

2.2 Fine Particulate Control

Present New Source Performance Standards for utility coal-fired boilers limit particulate emissions to 0.03 lb/million Btu and require 20% or lower opacity. The particulate control device removal efficiency required to meet this standard varies from about 99% to 99.9%, depending on the heating value and ash content of the coal. Electrostatic precipitators and fabric filters are the technologies that have most often been employed to meet the current standard. Although the best proven control technology for fine particulate matter appears to be fabric filtration, if properly designed, both of these technologies have been successful, in most cases, in meeting the current standard. However, the removal efficiency of both electrostatic precipitators and baghouses is significantly reduced for fine particles less than 2 micrometers. Furthermore, present emission standards do not adequately address such fine particle emissions. Emissions of fine particles are of concern because these particles can be deposited in the lower respiratory system through normal breathing. The potential problem is further compounded because hazardous trace elements such as selenium and arsenic are known to be concentrated on such fine particles. Control device removal efficiency is lowest for respirable particles, so a situation exists where the potentially most hazardous particles from coal combustion are collected with the lowest removal efficiency. In addition to potentially causing adverse health effects, fine particle emissions have an impact on atmospheric visibility. Particles that are the most efficient at scattering light are in the 0.2 to 2 micrometer range. These particles do not readily settle out of the atmosphere and are subject to long-range transport. When present in sufficient concentrations, these fine particles will cause serious visibility impairment. Therefore, the emission of fine particles is an issue because of potential adverse health effects and visibility impairment in the atmosphere.

Previous results at EERC showed that fine respirable particulate emissions could be reduced by up to 4 orders of magnitude by injecting small amounts of ammonia and SO_3 upstream of a baghouse (5-11). This corresponded to an increase in collection efficiency, for some difficult-to-collect ashes, from 90% to 99.999%. Emissions in some tests were less than ambient particulate levels in the atmosphere. Along with reduced particulate emissions, baghouse pressure drop was also reduced, making the process more economical. With some coals, pressure drop was reduced by 75%. Conditioning would add about 9% to the cost of operating a conventional reverse-gas baghouse, but this cost could be more than recovered if pressure drop and/or baghouse size were reduced.

The conditioning agents change the cohesive properties of the ash particles which reduces the seepage of dust through the fabric and facilitates the bridging of pinholes, inhibiting direct particle penetration. At the same time, a more porous dust cake is formed which results in reduced baghouse pressure drop. A review of penetration mechanisms shows that there is a theoretical basis for lower emissions with increased bulk cohesion (11). Pressure drop reduction as a result of conditioning is attributed to an increase in dust cake porosity, as theoretical and empirical models predict.

A major research need in further developing this technology is to quantify the cohesive strength of fly ash and reentrainment potential from an ash surface. Methods are available to measure the shear or tensile strength of bulk powders (12,13), but many of these tests were developed for soil

mechanics studies and may not accurately describe the behavior of fine powders such as fly ash. There is a need to test existing methods and select or develop a reliable method to measure cohesive strength. Further, the measured cohesive strength should be correlated with other ash properties to understand which ash properties control cohesive strength and to help understand how ash properties affect fine particle emissions from fabric filters.

3.0 GOALS AND OBJECTIVES

The objective of the Department of Energy's (DOE's) Flue Gas Cleanup Program, under the direction of the Pittsburgh Energy Technology Center (PETC), is to promote the widespread use of coal. This is to be accomplished by providing the technology necessary for utilization of coal in an environmentally and economically acceptable manner. The program addresses the reduction of acid rain precursor emissions as well as developing technologies with the potential to meet more stringent emissions control requirements for SO_2, NO_x, and particulate matter.

Activities within the Energy & Environmental Research Center's (EERC's) Cooperative Agreement Flue Gas Cleanup project address both the advanced NO_x control and fine particulate control areas of the DOE Flue Gas Cleanup Program. Specific activities involve the development of a catalytic fabric filter for NO_x and particulate control and methods to measure the cohesive strength and reentrainment potential of fly ashes relative to fine particle emissions from fabric filters.

3.1 Catalytic Fabric Filtration

The overall objective of the catalytic fabric filter effort is the development of a catalyst-coated fabric filter for NO_x and particulate control that will provide high removal efficiency of NO_x and particulate matter, acceptably long bag and catalyst life, and economic savings over a conventional SCR system and baghouse. Specific goals of the program are to develop a catalytic fabric that will provide:

1. 90% NO_x removal with <25 ppm ammonia slip.
2. A particulate removal efficiency >99.5%.
3. A bag/catalyst life of >1 year.
4. A 20% cost savings over conventional baghouse and SCR control technology.
5. Compatibility with SO_2 removal systems.
6. A nonhazardous waste material.

The experimental approach to meeting the stated objectives for development of the catalyst-coated fabric filter involves further fabric and catalyst development, testing of the product at three levels, and selection of the best fabrics for longer-term durability testing. The work is divided into four

tasks (Tasks A-D). Owens-Corning Fiberglas Corp. (OCF) will prepare and provide, at no cost to the program, catalyst-coated fabric samples and filter bags made from catalyst-coated fabric for use in the test program.

Task A - Catalyst/Fabric Development. Even though promising results were obtained in the early work funded by OCF, a continued effort was needed to further develop the product that would give the best combination of high NO_x removal capability, low ammonia slip, high particulate removal efficiency, and long catalyst/bag life. Specific parametric tests were conducted in which the fabric weave, coating composition, and coating process were adjusted to develop acceptable fabrics for further testing. Task A, the first level of screening, was employed to test the activity of the catalyst-coated fabric in a simulated flue gas environment using a small fabric filter holder. Data generated from the system included NO_x removal efficiency, ammonia slip, and SO_3 production. Several fabric samples from this development work were chosen for further evaluation in Task B. Task A was essentially completed during the project year, April 1988-June 1989; however, a small effort is planned for each of the next three years to support larger-scale development activities, if additional fabric screening is needed. This work will be funded as part of a competitive award from DOE-PETC to begin pilot-scale evaluation of catalyst-coated filter bags. Further development of the catalytic fabric filter concept will be minimal and eventually deleted from the Cooperative Agreement Flue Gas Cleanup project.

Task B - Fabric Screening Tests. Task B was designed to further evaluate fabric samples developed in Task A while filtering fly ash from a pulverized coal-fired combustion source. Fabric samples were tested under actual flue gas conditions (e.g., 650°F, fly ash and SO_x present) to determine the effect of coal type/fly ash on catalytic activity. It is critical that the fabric be tested in an actual flue gas stream produced from the combustion of coal, because submicron particles, volatile species, and trace elements are present that might affect the catalyst. Testing in a simulated flue gas stream with reentrained fly ash would not produce the same effect, since volatile species would not be present, and submicron fly ash particles are not easily reentrained as separate particles. Task B testing included the use of four different coals and the measurement of NO_x removal efficiency, ammonia slip, SO_3 production, and particulate removal efficiency. Since the slipstream sample system used fabric swatches of <1.0 ft^2, the cost of making multiple sets of full bags was avoided. Task B allowed the testing of a maximum number of samples in an actual flue gas environment at a minimum cost. The best performing fabric samples will be selected from Task B results for further evaluation in full bag tests. Task B was initiated and essentially completed in the past program year beginning July 1, 1989, and ending June 30, 1990. Two additional fabric screening tests are planned for the next project year (July 1990-June 1991) in conjunction with the setup and testing of a nitrous oxide (N_2O) analyzer.

Task C - Bag Evaluation and Parametric Tests. Task C is the second level of fabric testing in the proposed work. Up to five of the best performing fabrics in Tasks A and B will be made into bags and tested in a baghouse. The baghouse will filter fly ash from a pilot-scale, pulverized coal-fired combustor during 100-hour tests. Test parameters will include ammonia/NO_x molar ratio, air-to-cloth ratio, temperature, cleaning mode, and coal type. Four coals were selected for Tasks B and C during the past year. It is important that several coals with different properties are included in the

evaluation process, since the level of submicron particles, volatile trace elements, and SO_2/SO_3 ratio are highly dependent on the coal and may have varying effects on the catalyst-coated fabric. In addition, particulate removal efficiency in a fabric filter is coal specific; therefore, tests of particulate penetration must include several coals. At the completion of Task C, an assessment of the technology will be made to determine if longer-term durability testing of the fabric will proceed or if further fabric development is needed. Task C will start in the summer of 1991 and will be funded as part of a competitive award from DOE-PETC to begin pilot-scale evaluation of catalyst-coated filter bags. Pilot-scale development activities associated with the catalytic fabric filter concept will not be included in future project plans for the Cooperative Agreement Flue Gas Cleanup project.

Task D - Bag Durability and Process Assessment. Task D will proceed if Task C results are satisfactory. A fabric, selection based on the results of Tasks A, B, and C, will be evaluated for durability in a 500-hour test. The primary purpose of this test is to evaluate the durability of the fabric and catalyst in longer-term testing with multiple cleaning cycles and dust cake buildup on the fabric. Following the 500-hour test, an economic and technical assessment of the process, along with recommendations for further development, will be completed as part of Task D. Task D will be performed as part of a competitive award from DOE-PETC.

3.2 Fine Particulate Control

The general objective of the fine particulate control effort (Task E) is to develop methods to help characterize, control, and model fine particulate emissions from a fabric filter. Characterization efforts include the development of methods to measure the cohesive strength and reentrainment potential of fly ashes. Control and modeling efforts involve relating these parameters to the level of fine particle emissions from fabric filters. Specific goals for the past year have included the following:

1. Evaluate existing methods and select or develop reliable methods to measure the cohesive strength of fly ash.

2. Correlate measured cohesive strength with other ash properties such as particle size, particle shape, surface area, porosity, and ash chemistry.

3. Measure the reentrainment potential of ash from the surface of a fly ash filter cake or bulk fly ash and relate it to the measured cohesive strength.

4.0 ACCOMPLISHMENTS

4.1 Catalytic Fabric Filtration

The purpose of Task B was to evaluate eight of the best performing fabrics from Task A, while filtering fly ash from a pulverized coal-fired combustion facility. In an actual flue gas stream produced from the combustion of coal (unlike simulated flue gas), submicron particles, volatile species, and trace elements are present that might affect the catalyst. The criteria

for selecting the fabrics were high NO_x removal efficiency and/or low ammonia slip based on Task A results. Fabric samples selected for evaluation are identified in Table 1. A detailed description of each of these fabrics was presented in the Annual Project Report for April 1988 through June 1989 (3). Four coals were selected for use during Task B activities: a medium-sulfur, washed Illinois #6 bituminous; a high-sulfur Pyro Kentucky bituminous; a Jacobs Ranch subbituminous; and a South Hallsville, Texas, lignite. The ultimate and proximate analyses for each of the coals are presented in Table 2. The washed Illinois #6 bituminous coal was used as the baseline coal for the Task B tests.

Each of the eight fabrics was tested at air-to-cloth ratios of 2, 3, 4, and 6 ft/min with the baseline coal (washed Illinois #6). Ammonia slip and SO_3 measurements were made at each air-to-cloth ratio, with the ammonia/NO_x molar ratio held constant at 0.9. Following these tests, Fabrics #2 and #13 were selected to be tested using the remaining three coals. For the first 6 hours of the test, the air-to-cloth ratio was held constant at 3 ft/min. However, at the end of each test, the air-to-cloth ratio was then adjusted to 2 ft/min for 1 hour, followed by a change to 4 ft/min also for 1 hour. Again the ammonia/NO_x molar ratio was 0.9.

4.1.1 Description of Facilities and Procedures

The EERC particulate test combustor (PTC), shown in Figure 1, was designed for studies of flue gas emission control and particulate characterization. The combustor can be fired using natural gas or pulverized coal. When burning pulverized coal, the resultant fly ash is representative of that produced in full-scale pc-fired boilers. The mean residence time of a particle in the combustor is three seconds, based on the superficial gas velocity. The combustion chamber is 2 feet in diameter and 9 feet high, with a heat input of approximately 550,000 Btu/hr. Flue gas flow rates are measured using an orifice plate and an Annubar flow element and are typically 130 scfm. To protect the ID fan and to control particulate emissions, the shaker chamber of a pilot-scale baghouse was used during operation of the PTC. A stable ammonia injection rate was maintained with a calibrated mass flow controller.

To minimize the amount of construction necessary prior to testing, the 0.8 ft^2 fabric filter holder and oven used in Task A were used as part of the slipstream system in Task B. However, some minor modifications of the flue gas piping were necessary to facilitate operation and to ensure that the flue gas entering the slipstream sampler was at a minimum of 650°F. The slipstream sample system was designed and constructed such that flue gas produced from the PTC was drawn through the catalyst-coated fabric sample at the proper air-to-cloth ratio and measured using a calibrated orifice. After the fabric filter, the gas flow was split three ways. The first stream, about 10 scfh, was directed through a heat-traced line to a sample conditioner followed by the flue gas analyzers. The second stream, approximately 20 scfh, was used to measure either the ammonia slip or the concentration of SO_3 in the flue gas. The balance of the flue gas went to a gas pump and dry gas meter for control of the total system flow. A schematic of the slipstream sample system is shown in Figure 2.

TABLE 1

FABRICS SELECTED FOR EVALUATION IN TASK B
BASED ON TASK A RESULTS

Fabric ID No.	NO_x Removal Efficiency (%)	Ammonia Slip (ppm)
2	92.6	35
3	91.3	53
4	76.6	24
5	83.8	3
7	87.7	9
13	61.7	8
14	91.3	25
15	90.0	44

TABLE 2

ANALYSES OF COAL USED IN TASK B
(On an As-Received Basis)

	Washed Illinois #6	Kentucky Pyro	Wyoming Jacobs Ranch	South Hallsville
Coal Type	Bituminous	Bituminous	Subbituminous	Lignite
Proximate Analysis (%)				
Moisture	13.7	5.9	23.1	36.8
Volatile Matter	32.8	31.7	33.0	23.6
Fixed Carbon	43.2	48.1	38.5	29.8
Ash	10.3	13.3	5.5	9.6
Ultimate Analysis (%)				
Hydrogen	5.8	5.5	6.8	6.6
Carbon	61.0	65.6	52.5	39.8
Nitrogen	1.0	1.3	0.7	0.5
Sulfur	2.7	4.6	0.3	1.3
Oxygen (Diff.)	19.3	9.7	34.3	42.2
Ash	10.3	13.3	5.5	9.6
Heating Value (Btu/lb)	10,819	11,857	9,129	6,719

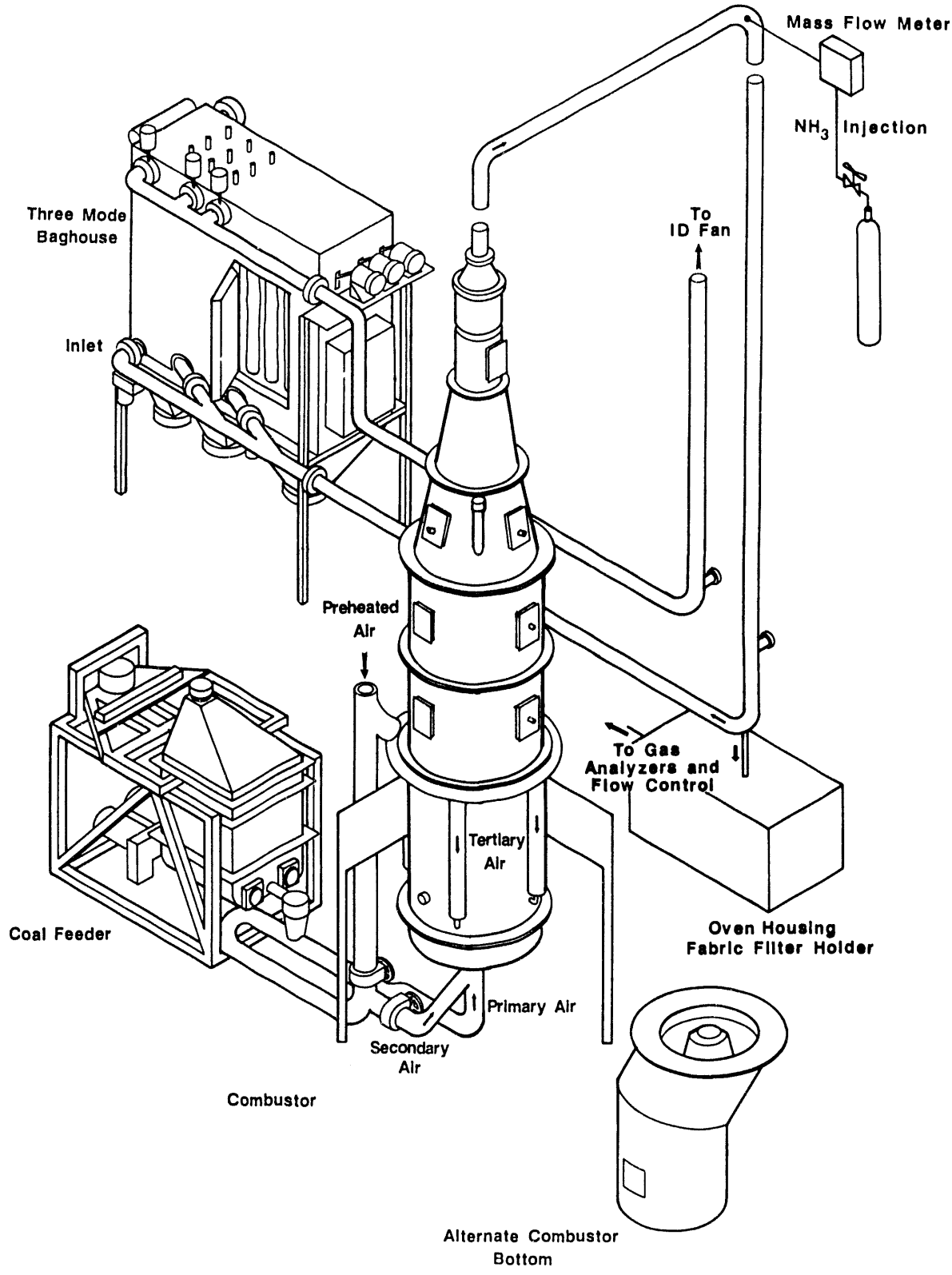

Figure 1. Particulate test combustor (PTC): pulverized coal- or gas-fired at 550,000 Btu/hr.

After installation of the slipstream sample system, a short shakedown test was conducted, firing natural gas. The purpose of the test was to determine the best method for obtaining a flue gas temperature of 700°F at the inlet to the slipstream sample system and, at the same time, prevent the baghouse temperature from exceeding 500°F. In addition, the overall operation of the slipstream sample system was evaluated. By using the proper number of heat exchangers and insulating the flue gas piping, the proper temperatures were obtained. The slipstream sample system operated as expected, and no changes to the apparatus were needed.

Continuous on-line flue gas analyzers were used to monitor carbon dioxide, oxygen, sulfur dioxide, and oxides of nitrogen at the combustor exit and the inlet and outlet of the fabric filter holder. Ammonia slip measurements were made by bubbling the flue gas through a solution of 0.1 N sulfuric acid and then measuring the ammonia in the solution using a modification of the Kjeldahl method. The selective condensation technique (14) was used to collect SO_3 from the flue gas, and then the concentration was determined by titration. In addition, HCl measurements were made for the Pyro Kentucky bituminous coal and the South Hallsville, Texas, lignite. HCl is collected by bubbling the flue gas through a water impinger train and then measuring the chloride ion concentration using a selective ion electrode.

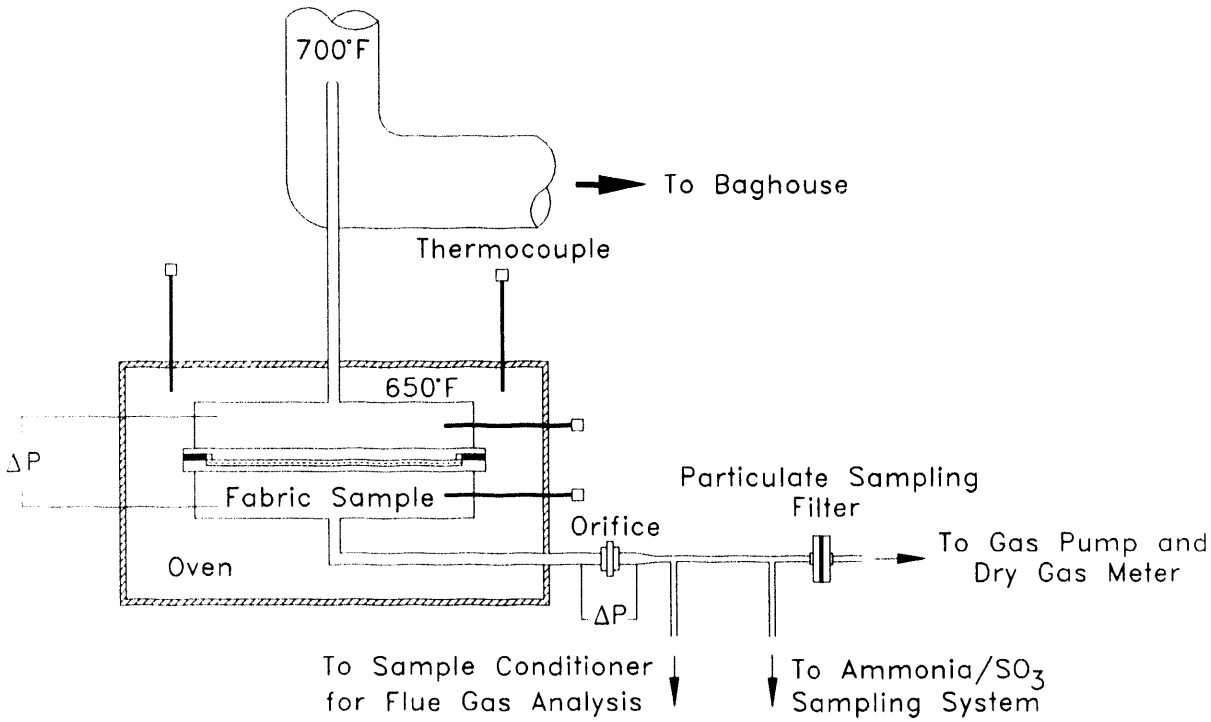

Figure 2. Slipstream sample system.

Pressure drop across the filter was measured continuously. When it was necessary to clean the filter to reduce the pressure drop, the gas flow through the fabric filter was reversed, causing the dust cake to be disturbed. Although the dust was not actually removed from the fabric, this approach was sufficient to keep the pressure drop at a manageable level.

Particulate collection efficiency was approximated for each fabric sample. This was accomplished by calculating an inlet mass loading based on the measured coal ash content and assuming 60% of the coal ash reached the sampling location as fly ash in the pilot-scale combustion system. In addition, for one of the tests, a measurement of actual particulate mass loading on the fabric filter was made. The outlet mass loading was determined by using a small filter to collect fly ash from a portion of the flue gas stream exiting the oven which held the catalyst-coated fabric.

Surface area and vanadium concentrations were determined for each of the fabric samples tested. The surface area was measured using a BET surface area analyzer. The vanadium concentration on the fabric was measured by first weighing a small amount of the catalyst-coated fabric and then dissolving it in a solution of ultrapure hydrofluoric acid followed by a solution of ultrapure aqua regia. The liquid was then diluted to 100 ml with deionized water and analyzed for vanadium using atomic absorption techniques.

4.1.2 Fabric Screening

The intent of the fabric screening tests was to evaluate the effect of air-to-cloth ratio (2, 3, 4, and 6 ft/min) on each of the catalyst-coated fabric samples at a single temperature (650°F) and ammonia/NO_x molar ratio (0.9). However, an error was made in calculating the orifice coefficient for determining the flue gas flow rate in the pilot-scale combustion system. This error resulted in a calculated total flue gas flow rate higher than the actual flue gas flow rate for the pilot-scale combustion system. Therefore, the ammonia/NO_x molar ratio for several of the initial tests was closer to 1.1 than the 0.9 value desired. Although this error resulted in higher NO_x removal and ammonia slip values and lower SO_3 values than would have been observed at an ammonia/NO_x molar ratio of 0.9, the data were useful for comparison of fabric performance. In addition, tests with Fabric #2 were repeated at an ammonia/NO_x molar ratio of 0.9 to aid in the comparison.

The results of the fabric screening tests for the eight selected fabrics are presented in Table 3. These results are consistent with the values reported for Task A (3). The only exception was Fabric #3, which provided 91% NO_x removal efficiency in Task A compared to only 70% during the Task B test period at an air-to-cloth ratio of 2 ft/min. EERC personnel contacted OCF personnel to discuss possible reasons for the poor performance of Fabric #3. During the discussion, it was determined that low ambient temperature may have affected the hydrolysis reaction during the coating process, carried out in a ventilated hood, resulting in nonuniform catalyst coating. This would explain the low NO_x removal observed during Task B tests. Figure 3 is a SEM micrograph of Fabric #3 showing a nonuniform catalyst coating. Several of the fibers (lower-left portion of the photograph) appear to have no catalyst coating.

TABLE 3

RESULTS FROM TASK B--BENCH-SCALE FABRIC SCREENING TESTS[a]

Fabric No.	A/C Ratio (ft/min)	NH_3/NO_x Molar Ratio	NO_x Inlet (ppm)	NO_x Outlet (ppm)	NO_x Removal Efficiency (%)	Ammonia Slip (ppm)	SO_3 Conc.[b] (ppm)	Flue Gas Moisture (%)	Particulate Removal Efficiency (%)
2	2	1.1	765	20	97.4	187	4		
2	3	1.1	716	38	94.7	63	4		
2	4	1.1	740	83	88.8	129	3	ND[c]	99.8
2	4.5	1.1	735	64	91.3	121	3		
2	2	0.9	540	58	89.3	5	2		
2	3	0.9	550	83	84.9	7	2		
2	4	0.9	590	112	81.0	22	124	9.3	99.8
2	6	0.9	630	175	72.2	76	1		
3	2	0.9	760	226	70.3	ND	ND		
3	4	0.9	710	390	45.1	ND	ND	ND	90.4
3	6	0.9	720	490	31.9	357	5		
4	2	0.9	715	171	76.1	87	1		
4	3	0.9	695	235	66.2	127	2		
4	4	0.9	675	310	54.1	179	2	8.9	99.5
4	6	0.9	645	436	32.4	288	266		
5	2	0.9	730	90	87.7	28	2		
5	3	0.9	700	125	82.1	54	1		
5	4	0.9	760	190	75.0	76	1	8.4	99.9
5	6	0.9	730	305	58.2	163	60		
7	2	0.9	700	75	89.3	4	ND		
7	3	0.9	675	95	85.9	13	ND		
7	4	0.9	650	175	73.1	33	ND	8.6	99.8
7	6	0.9	660	200	69.7	50	1216		
13	2	1.1	673	34	94.9	64	4		
13	3	1.1	686	64	90.7	58	2		
13	4	1.1	688	126	81.7	88	169	8.4	99.4
13	6	1.1	671	209	68.9	108	115		
14	2	1.1	703	89	87.3	107	1		
14	3	1.1	729	151	79.3	153	2		
14	4	1.1	772	228	70.5	256	2	7.8	99.8
14	6	1.1	838	433	48.3	179	4		
15	2	1.1	847	40	95.3	57	2		
15	3	1.1	789	68	91.4	58	1		
15	4	1.1	761	98	87.1	104	1	8.9	99.9
15	6	1.1	656	193	70.6	122	4		

[a] Each catalyst-coated fabric sample was evaluated using a slipstream of flue gas from a pc-fired pilot-scale combustor firing a washed Illinois #6 bituminous coal.

[b] Actual SO_3 concentrations may be higher than the indicated values due to interference by ammonia.

[c] "ND" denotes data not available due to problems encountered with the sampling system.

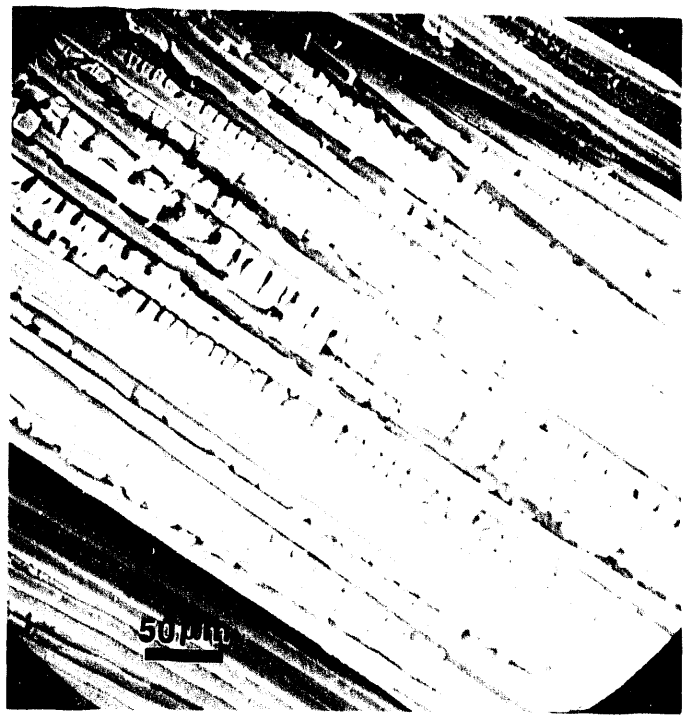

Figure 3. SEM micrograph of Fabric #3 showing nonuniform catalyst coating.

Fabric #3 also demonstrated poor particulate control efficiency when compared to the seven other fabric samples, 90.4% versus >99%. Following termination of the test, the filter holder was opened, and a large number of pinholes were observed in Fabric #3's dust cake. In addition, the clean side of the fabric sample collected dust at the pinhole sites. Poor particulate collection is consistent with the pinhole formation observed and may have been a result of the inconsistent catalyst coating. Pinhole formation probably caused flue gas channeling which may have contributed to poor NO_x reduction and high ammonia slip. Figure 4 is a photograph of the dust cake showing several pinholes that formed.

Figures 5 through 12 show the effect of air-to-cloth ratio on NO_x removal efficiency with time. As expected, there was a marked decrease in NO_x removal efficiency with increased air-to-cloth ratio. Although there was some variability in the operation of the combustion system, NO_x removal efficiency was relatively constant with time. An upset in the sampling system occurred during the testing of Fabric #7 (Figure 9), causing water from an impinger train to back up on to the catalyst-coated fabric sample. This resulted in a temporary decrease in NO_x removal efficiency, as shown in Figure 9.

Fabric #2 appeared to demonstrate the best overall performance with respect to high NO_x removal, low ammonia slip, and low SO_3 production. Although Fabrics #13 and #15 also provided good NO_x removal efficiency, these fabric samples were tested at an ammonia/NO_x molar ratio of 1.1, resulting in higher

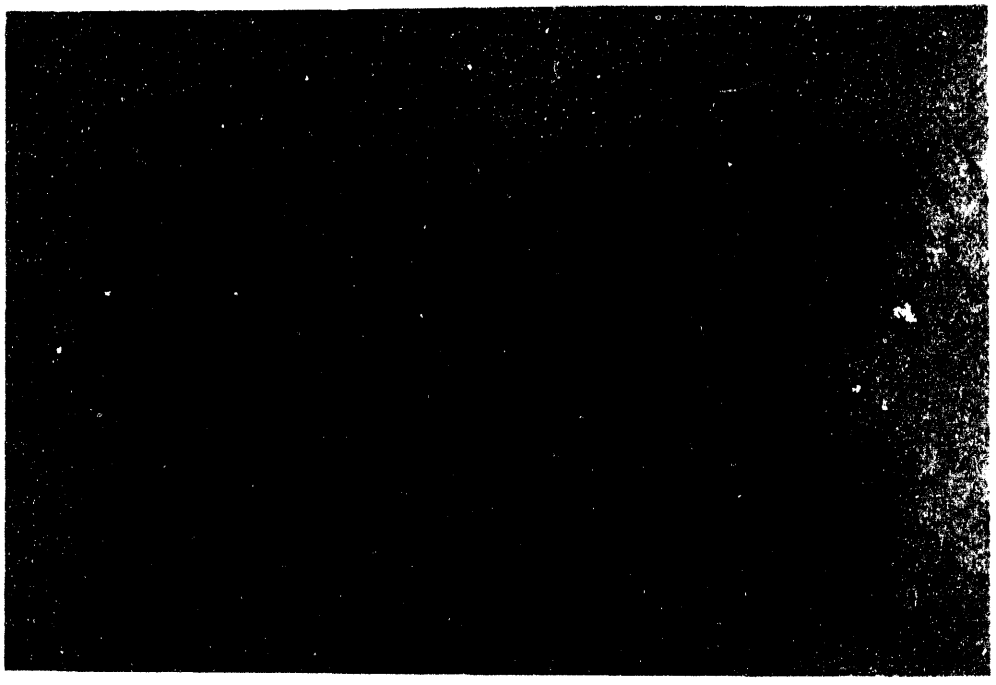

Figure 4. Photograph of pinholes observed on Fabric #3 after opening the filter holder.

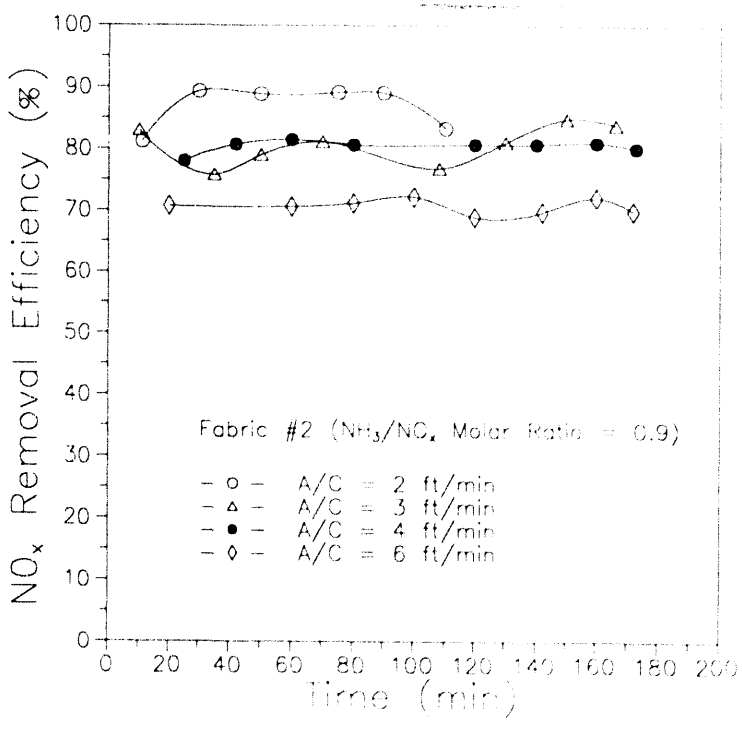

Figure 5. NO_x removal efficiency as a function of time and air-to-cloth ratio for Fabric #2.

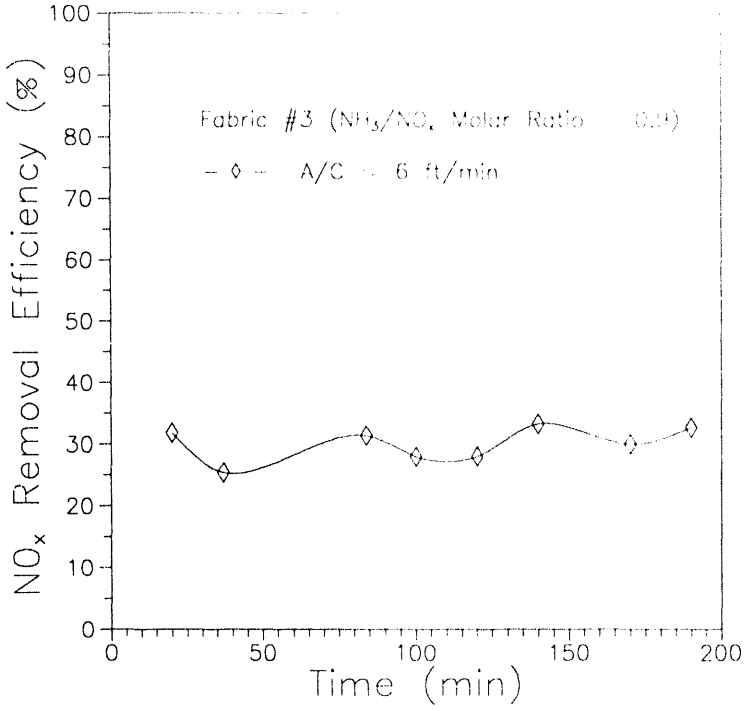

Figure 6. NO_x removal efficiency as a function of time and air-to-cloth ratio for Fabric #3.

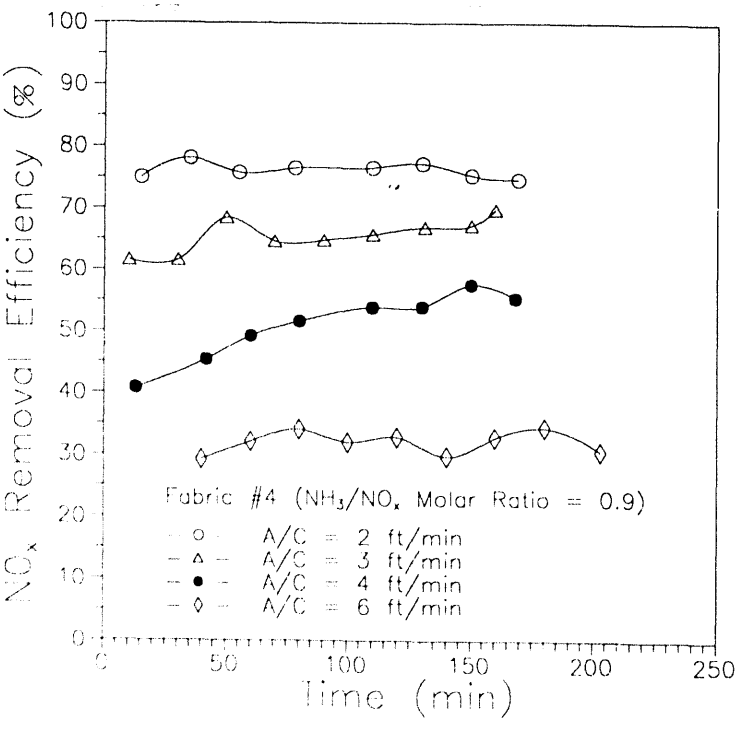

Figure 7. NO_x removal efficiency as a function of time and air-to-cloth ratio for Fabric #4.

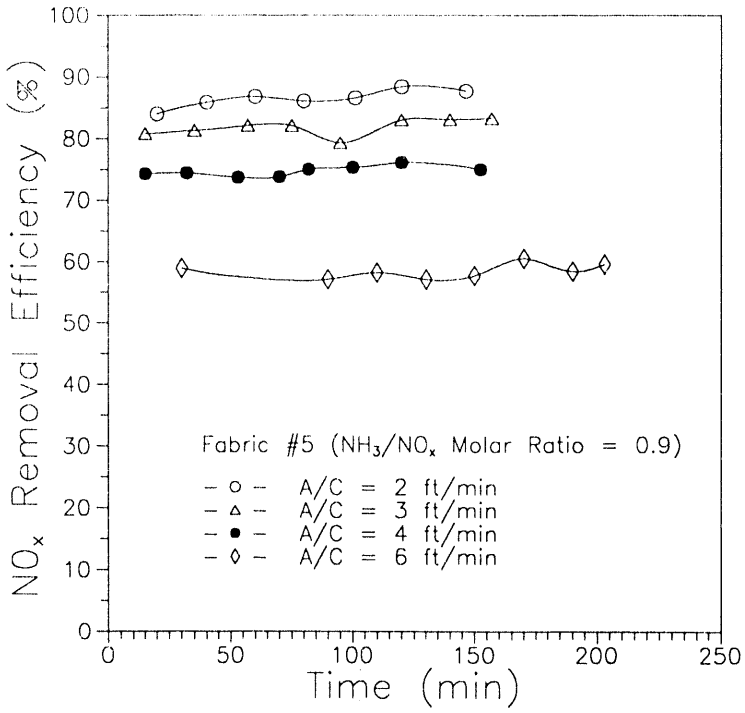

Figure 8. NO_x removal efficiency as a function of time and air-to-cloth ratio for Fabric #5.

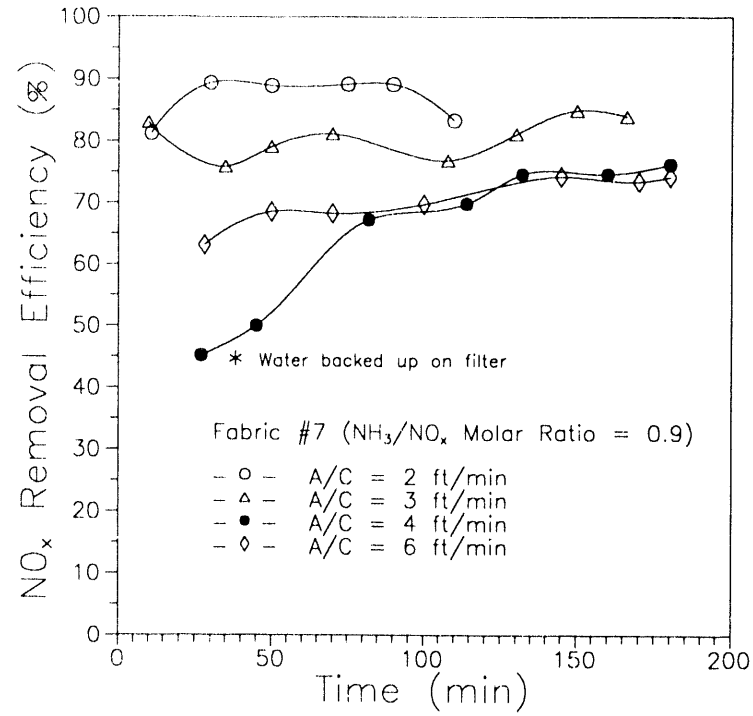

Figure 9. NO_x removal efficiency as a function of time and air-to-cloth ratio for Fabric #7.

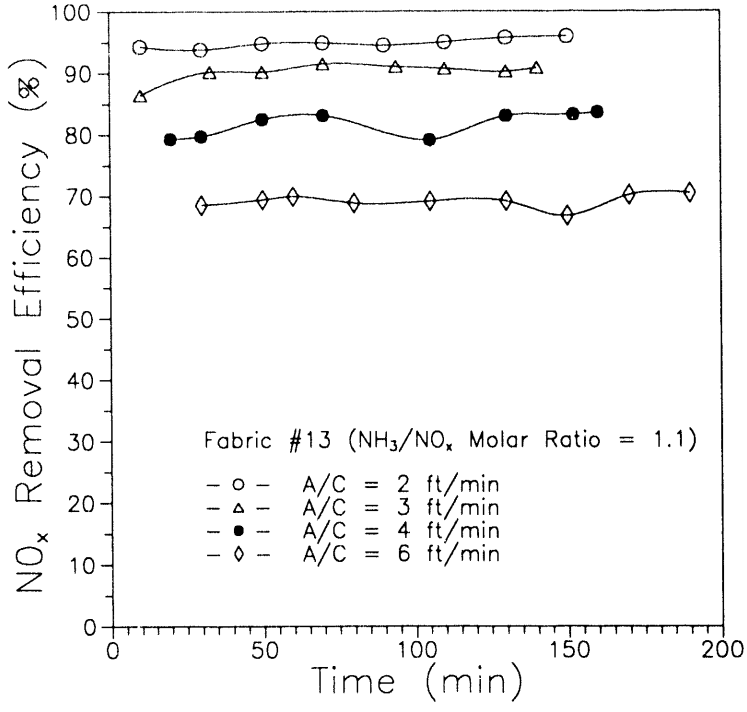

Figure 10. NO_x removal efficiency as a function of time and air-to-cloth ratio for Fabric #13.

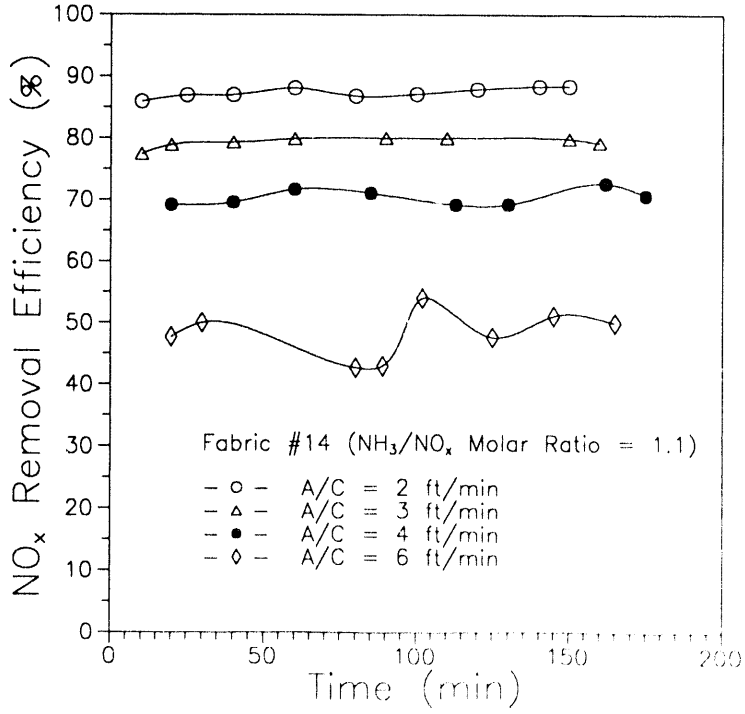

Figure 11. NO_x removal efficiency as a function of time and air-to-cloth ratio for Fabric #14.

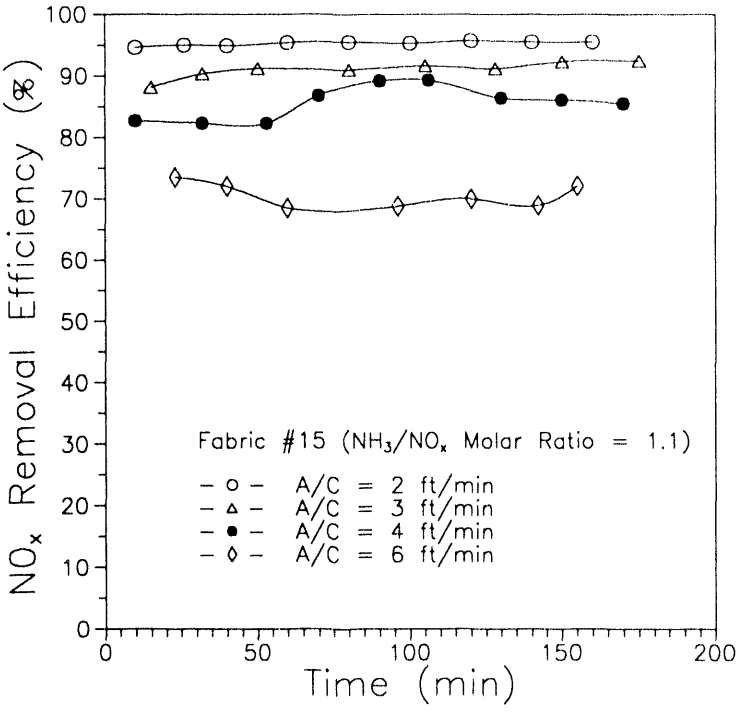

Figure 12. NO_x removal efficiency as a function of time and air-to-cloth ratio for Fabric #15.

ammonia slip values. From the data, it appears that the maximum air-to-cloth ratio that can be used and still obtain >85% NO_x removal efficiency is 3 ft/min. This is consistent with the bench-scale results in Task A. For all eight fabric samples, there was a marked decrease in catalyst-coated fabric performance at air-to-cloth ratios of 4 and 6 ft/min.

For every fabric sample, ammonia slip and SO_3 concentration measurements were made at each air-to-cloth ratio tested. Figure 13 shows NO_x removal efficiency as a function of ammonia slip for those fabrics tested at an ammonia/NO_x molar ratio of 0.9. Although there is some data scatter, the graph does show a correlation between ammonia slip and NO_x removal efficiency.

There is a concern that the vanadium catalyst in an SCR process, such as the catalyst-coated filter, will convert SO_2 to SO_3. High levels of SO_3 are considered to be a problem because of the possibility of corrosion and deposition in the air preheater. Although the SO_3 concentration in the flue gas was high for several of the tests, particularly at the high air-to-cloth ratios, in most cases the SO_3 concentration was very low, <5 ppm. This may be due to interference from ammonia. Some measurements of the SO_3 concentration in the flue gas were made with the ammonia turned off, and these data will be discussed later in the report. It is unclear at this time why a few of the test results showed high concentrations of SO_3.

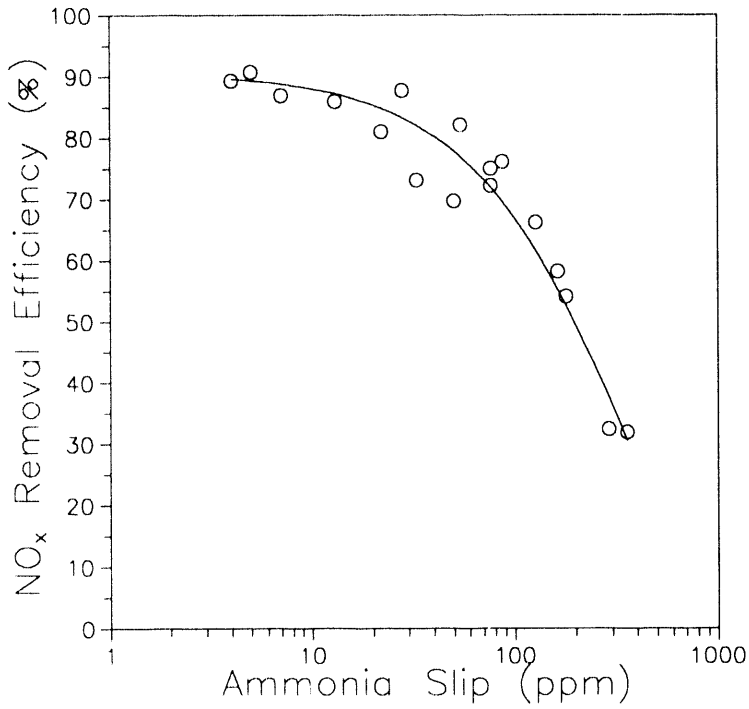

Figure 13. NO_x removal efficiency as a function of ammonia slip.

4.1.3 Effects of Coal Type on Catalyst-Coated Fabric Performance

Following completion of the fabric screening tests, Fabrics #2 and #13 were chosen to test the effects of coal type on catalyst-coated fabric performance. Both fabrics were tested using each of the three remaining coals (South Hallsville, Texas, lignite; Jacobs Ranch subbituminous; and a Pyro Kentucky bituminous) at a constant air-to-cloth ratio of 3 ft/min, an ammonia/NO_x molar ratio of 0.9, and a flue gas temperature of 650°F. Table 4 summarizes the results from these tests as well as data from the previous screening tests using the washed Illinois #6 bituminous coal. The data are also represented graphically in Figures 14 through 19.

Figure 14 shows that for Fabric #2, with the exception of the South Hallsville, Texas, lignite, there is very little difference in the NO_x removal efficiency as a function of coal type. South Hallsville, Texas, lignite is known to produce an ash that is difficult to collect in a fabric filter (8). Although no dust loading was obtained for this test, the backup filter plugged very quickly, and a large number of pinholes were present in the dust cake at the conclusion of the test, indicating reduced particulate collection efficiency and possible flue gas channeling. Pinholes result in localized areas of very high air-to-cloth ratios which, depending on the number and size of the pinholes, can result in decreased NO_x removal and increased particulate penetration.

TABLE 4

RESULTS FROM TASK B--EFFECTS OF COAL TYPE[a]

Fabric No.	A/C Ratio (ft/min)	NH_3/NO_x Molar Ratio	NO_x Inlet (ppm)	NO_x Outlet (ppm)	NO_x Removal Efficiency (%)	Ammonia Slip (ppm)	SO_3 Conc. (ppm)	HCl Conc. (ppm)	Flue Gas Moisture (%)	Particulate Removal Efficiency (%)
					Washed Illinois #6 Bituminous					
2	2	0.9	540	58	89.3					
2	3	0.9	535	81	84.9	7	2	----	9.3	99.8
2	4	0.9	590	112	81.0					
2	2	1.1	765	20	97.4	187	4			
2	3	1.1	716	38	94.7	63	4			
2	4	1.1	740	83	88.8	129	3	ND[b]		99.8
13	2	1.1	673	34	94.9					
13	3	1.1	686	64	90.7	58	2	----	8.4	99.4
13	4	1.1	688	126	81.7					
					Jacobs Ranch, Wyoming, Subbituminous					
2	2	0.9	785	59	92.5					
2	3	0.9	760	75	90.1	86	0	----	12.4	99.9
2	4	0.9	800	90	88.8					
13	2	0.9	645	80	87.6					
13	3	0.9	680	105	84.6	99	0	----	11.9	99.9
13	4	0.9	675	195	71.1					
					South Hallsville, Texas, Lignite					
2	3	0.9	900	175	80.6	121	1	17	----	----
13	2	0.9	820	110	86.6					
13	3	0.9	810	140	82.7	75	1	1	13.0	99.8
13	4	0.9	825	195	76.4					
					Pyro Kentucky Bituminous					
2	2	0.9	970	93	90.4					
2	3	0.9	930	130	86.0	10	1	----	8.0	99.7
2	4	0.9	925	178	80.8					
13	3	0.9	810	170	79.0	30	1	142	8.9	99.6

[a] Each catalyst-coated fabric sample was evaluated using a slipstream of flue gas from a pc-fired pilot-scale combustor.

[b] "ND" denotes data not available due to problems encountered with the sampling system.

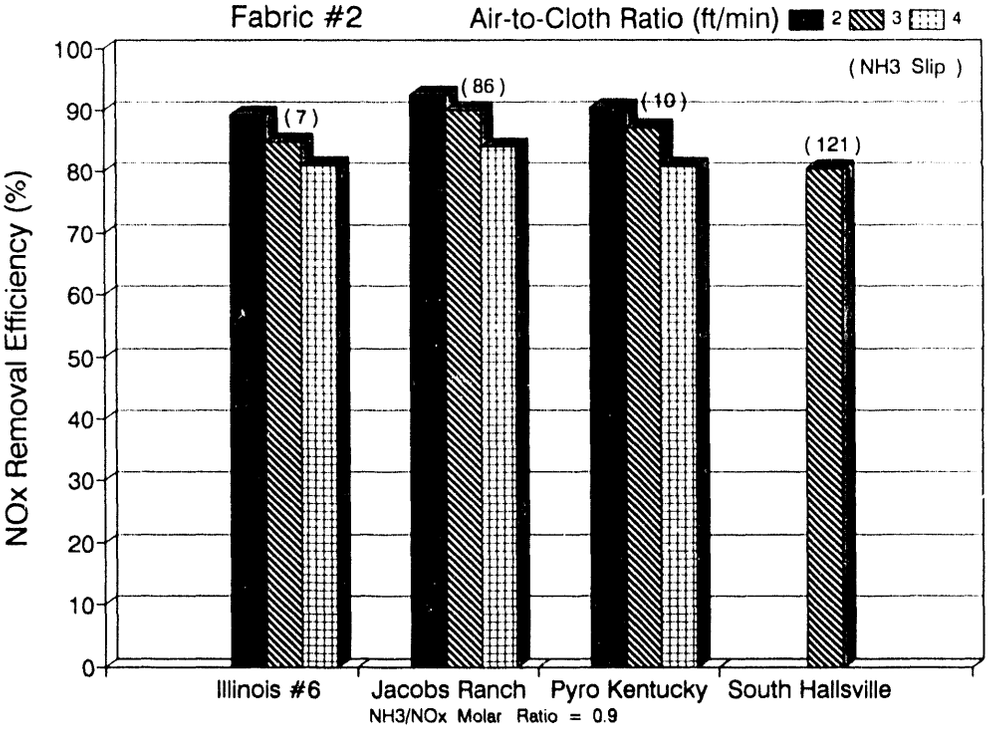

Figure 14. Comparison of the catalytic performance using four different coals for Fabric #2.

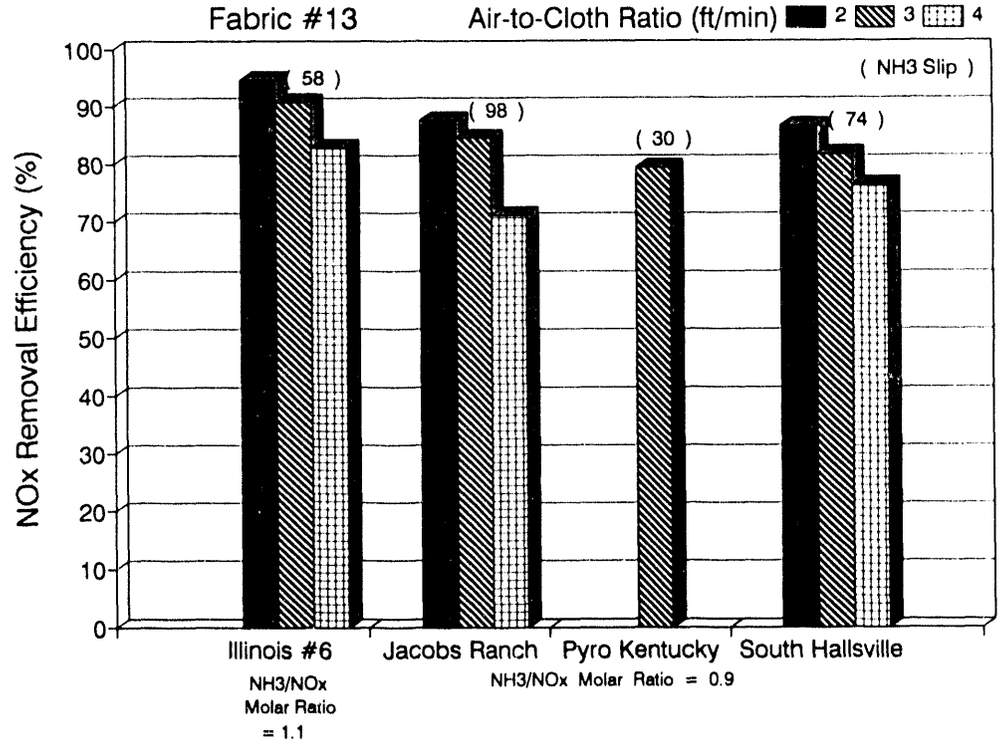

Figure 15. Comparison of the catalytic performance using four different coals for Fabric #13.

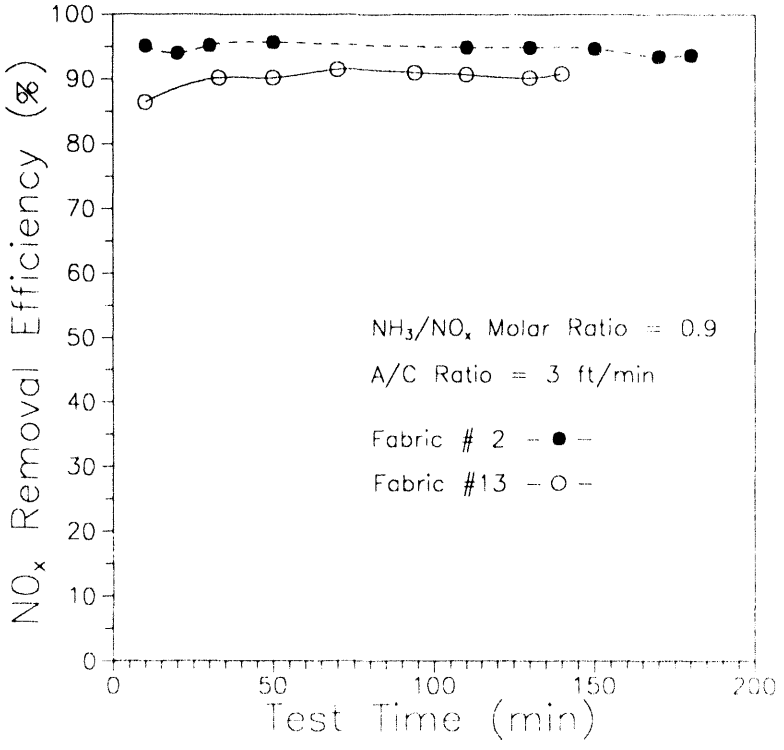

Figure 16. NO_x removal efficiency as a function of time, fabric, and air-to-cloth ratio for a washed Illinois #6 bituminous coal.

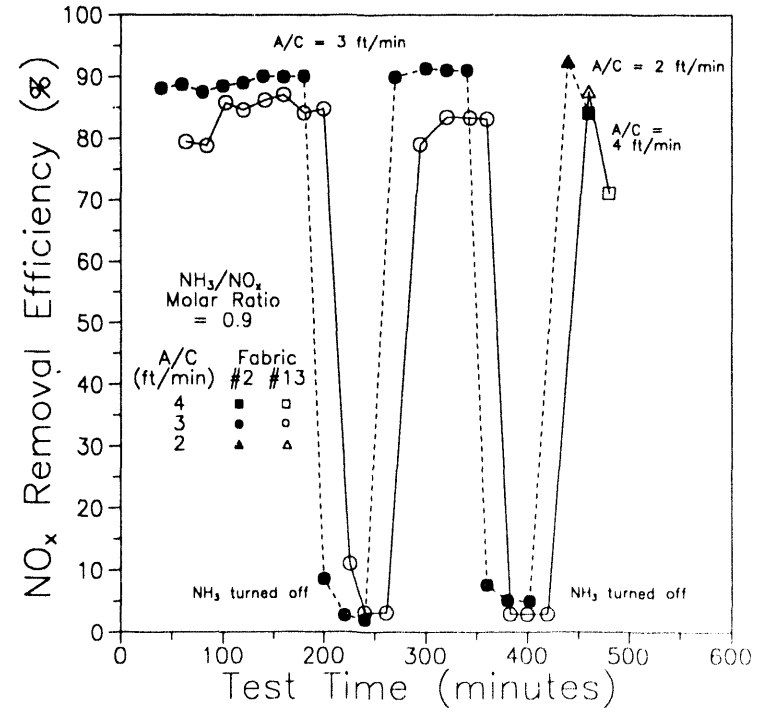

Figure 17. NO_x removal efficiency as a function of time, fabric, and air-to-cloth ratio for a Jacobs Ranch subbituminous coal.

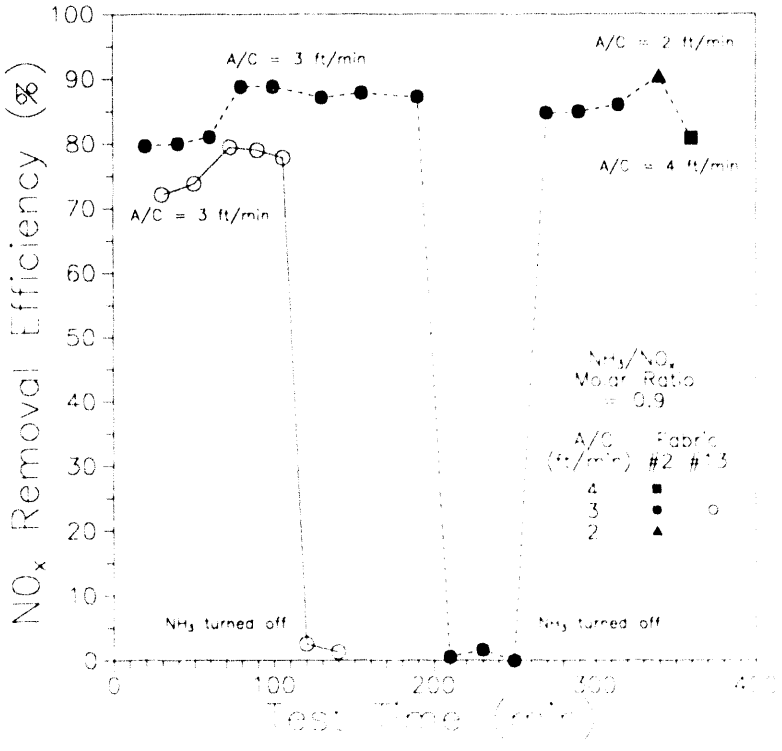

Figure 18. NO_x removal efficiency as a function of time, fabric, and air-to-cloth ratio for a Pyro Kentucky bituminous coal.

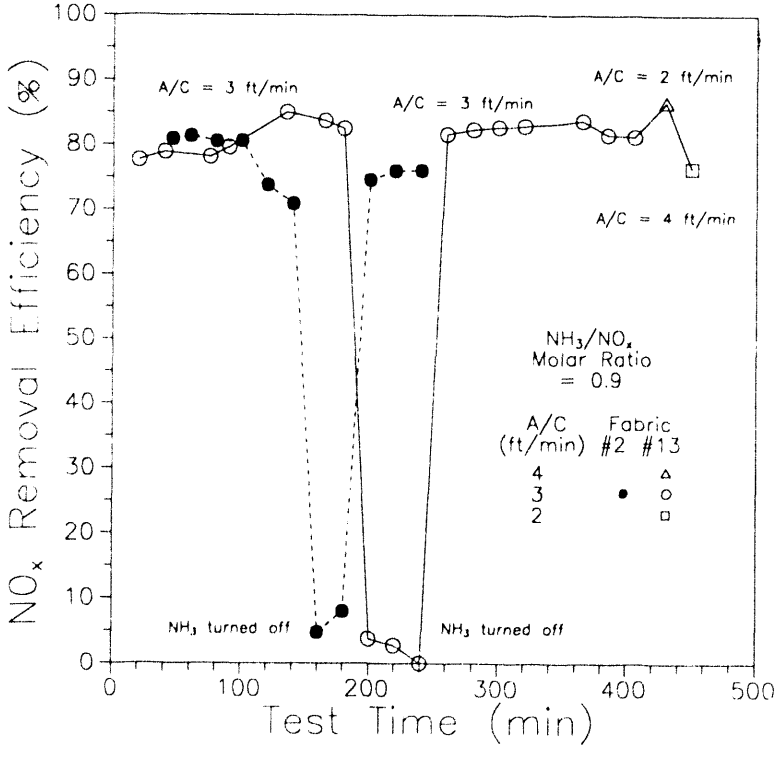

Figure 19. NO_x removal efficiency as a function of time, fabric, and air-to-cloth ratio for a South Hallsville, Texas, lignite.

The test using Fabric #13 (Figure 15) firing South Hallsville, Texas, lignite was more successful, as excessive pinholing did not occur. However, the NO_x removal efficiency was somewhat lower, about 83% compared to 86% and 90% for the Jacobs Ranch and Illinois #6 coals, respectively. The results using the Pyro Kentucky bituminous coal with Fabric #13 are suspect due to an upset in the pilot-scale combustion system. Excessive slagging resulted in an unstable flame in the burner, causing an early shutdown of this test.

Figures 16 through 19 compare the performance of Fabrics #2 and #13 for each of the four different coals. With the possible exception of the South Hallsville, Texas, lignite (Figure 17), Fabric #2 provided greater NO_x removal efficiency than Fabric #13.

Ammonia slip and SO_3 concentration measurements were made for each test. In addition, for the Pyro Kentucky bituminous coal, the concentration of HCl was measured due to high levels of chlorine in the coal (0.2%). As a baseline, an HCl measurement was also made when firing South Hallsville, Texas, lignite which has very low chlorine content. The ammonia slip was higher than would be expected for several of the tests. A possible explanation is the ammonia/NO_x molar ratio was not as constant as would have been desired. There was some instability in the combustion system which resulted in NO_x readings that were ± 50 ppm, and it was not always possible to adjust the ammonia flow rate to correct for this change.

To get a more accurate indication of the SO_3 concentration in the flue gas, the ammonia was turned off during the time when the SO_3 measurements were being made. During this time, the NO_x removal efficiency went to zero, as shown in Figures 16 through 19. Although the ammonia was not on, the SO_3 concentrations downstream of the catalyst-coated fabrics were extremely low (<2 ppm). This result was unexpected, especially for the high-sulfur (3800 ppm SO_2 in the flue gas) Pyro Kentucky bituminous coal.

As expected, the HCl concentration in the flue gas during the tests using Pyro Kentucky bituminous coal was high, 142 ppm. The calculated, theoretical flue gas value for a coal with a chlorine content of 0.2% was 149 ppm at similar flue gas conditions. In addition, two HCl measurements were made during the tests burning the South Hallsville, Texas, lignite which contains essentially no chlorine. The first test using Fabric #2 verified this, as the HCl concentration in the flue gas was <1 ppm. However, the HCl concentration in the flue gas for the second South Hallsville test with Fabric #13 was 17 ppm. This test was completed following a Pyro Kentucky test; therefore, the higher HCl value may have been a result of residual HCl absorbed on fly ash deposits in the duct.

4.1.4 Fabric Characterization

Table 5 presents the surface area and vanadium concentration for each of the fabrics tested. Both were measured prior to exposure to the flue gas and after completion of the reactivity tests. In all cases, except for Fabric #14, exposure of the fabric samples to flue gas resulted in a decrease in both the fabric's surface area and the fabric's vanadium concentration. However, in each case, the percentage decrease in surface area was substantially larger than the decrease in vanadium concentration. Figure 20 shows surface area as a function of vanadium concentration for both the exposed and unexposed fabrics. The two plots are anchored at the surface area determined for the

TABLE 5

VANADIUM CONCENTRATION AND BET SURFACE AREA
FOR EACH OF THE CATALYST-COATED FABRICS TESTED

	Vanadium[a]			Surface Area[b]		
Fabric No.	Unexposed[c] (mg/g)	Exposed (mg/g)	Change (%)	Unexposed (m^2/g)	Exposed (m^2/g)	Change (%)
Blank	0.03	---	---	0.56	----	----
2	9.1	9.0	1.1	9.50	6.19	34.8
2	8.4	8.3	1.2	10.68	5.11	52.2
3	4.7	3.7	21.3	3.31	1.54	53.5
4	4.7	4.2	10.6	4.28	2.02	52.8
5	5.5	5.4	1.8	5.79	3.74	35.4
7	7.6	6.3	17.1	6.62	2.74	58.6
13	6.8	6.1	10.3	5.76	4.04	29.9
13	8.4	8.0	4.8	6.52	4.00	38.7
14	3.4	3.6	-5.9	3.09	1.90	38.5
15	7.7	5.7	26.0	6.24	3.79	39.3

[a] Vanadium concentration is mg vanadium per g of coated fabric.
[b] Fabric surface area is m^2 per g of coated fabric (BET surface area).
[c] Unexposed and exposed refer to exposure to flue gas.

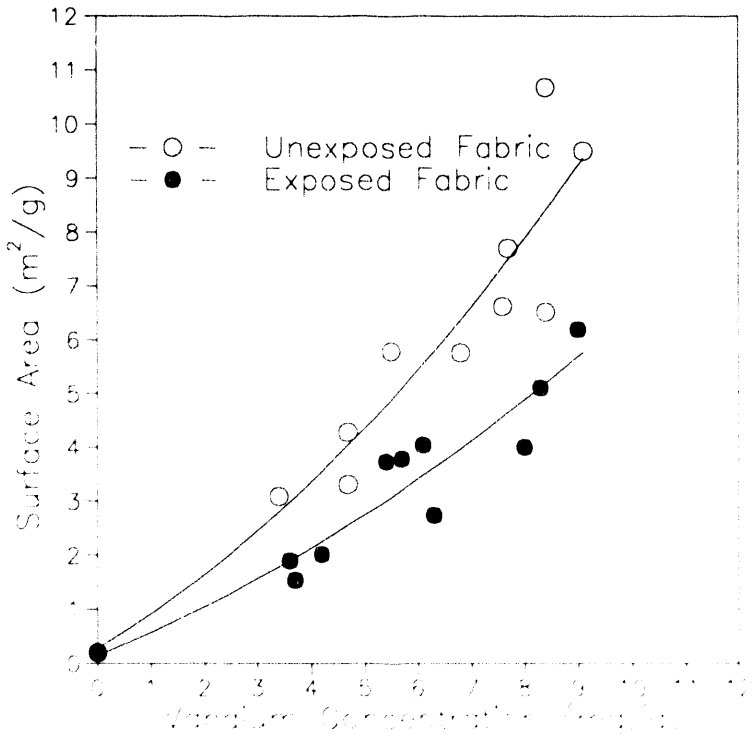

Figure 20. BET surface area of both exposed and unexposed catalytic fabrics as a function of vanadium concentration.

blank fabric. The graph and table tend to support the conclusion that a large percentage of the catalyst pore structure is located at or near the surface. During use, some of the surface catalyst is lost, resulting in a greater percentage decrease in surface area.

BET surface area data for the fabric samples exposed to flue gas are plotted as a function of ammonia slip in Figure 21. The figure includes data from Task A as presented in the previous annual report (3). Task B data only included the fabrics that were tested at an ammonia/NO_x molar ratio of 0.9 and at an air-to-cloth ratio of 2 ft/min, so that comparisons can be made to Task A results. Although there is some data scatter, the conclusions that were made previously are still valid. Fabric samples having a surface area of 6 to 9 m^2/g resulted in low ammonia slip (<10 ppm). Surface area values between 4 and 6 m^2/g resulted in moderate ammonia slip (10 to 50 ppm). For those fabrics with a surface area below 4 m^2/g, ammonia slip values increased exponentially.

Figure 22 shows that both the concentration of vanadium on the fabric and the BET surface area correlate strongly with NO_x removal efficiency. Although other factors such as weave texturization are also important, the data presented in the figure imply that, at an air-to-cloth ratio of 3 ft/min, a minimum concentration of 6 mg vanadium per gram of fabric and a surface area of about 4.5 m^2/g are necessary to achieve 85% NO_x reduction at an ammonia/NO_x molar ratio of 0.9. One surface area data point does not fit the curve. The data point represents Fabric #7 and a final determination concerning its validity has not been made.

Table 5 shows that two sets of samples of Fabrics #2 and #13 were used in Task B. The first set of fabric samples was used to complete the fabric screening tests with the Illinois #6 bituminous coal and the tests using the Jacobs Ranch subbituminous coal. However, after completing two tests with the Jacobs Ranch coal, the fabric samples were no longer useable due to excessive fraying. It was then necessary to obtain new fabric samples from OCF. There was a measurable difference in catalyst concentration between the first and second fabric samples. However, after the fabrics had been exposed to flue gas, the surface areas were essentially the same. The issue of quality control, with respect to the coating process, has not been specifically addressed in any of the work completed by EERC. A joint review of the recent data by EERC and OCF would be appropriate with respect to catalyst-coated fabric characteristics, the coating process, and quality control issues.

4.2 Fine Particulate Control

4.2.1 Summary of Fine Particulate Control work

The work in support of Task E consisted of the characterization of conditioned and baseline fly ash samples that were available from previous DOE-supported work at EERC (Contract No. DE-AC22-88PC88866). This activity was not intended to be a stand-alone effort, but was a logical follow-on to the previous Flue Gas Conditioning for Fabric Filter Performance Improvement project (final report completed December 1989 (15)).

The primary focus of the work has been to develop methods to measure the cohesive properties of fly ash and relate these properties to filtration

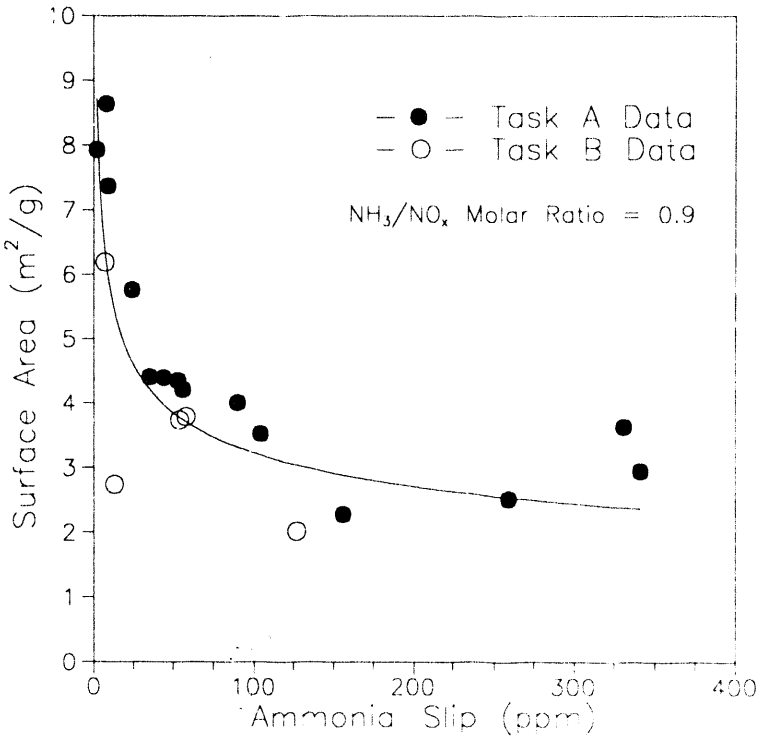

Figure 21. Surface area as a function of ammonia slip for both Task A and Task B results.

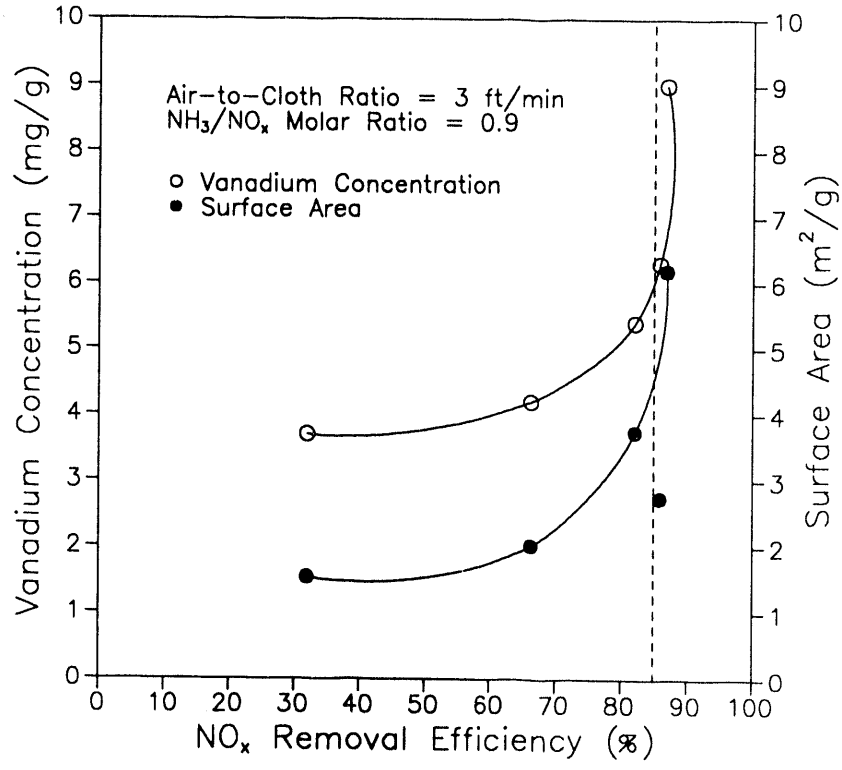

Figure 22. Vanadium concentration and BET surface area as a function of NO_x removal efficiency.

behavior. This information should lead to a better understanding of how fly ash properties affect fine particle emissions from fabric filters and of the conditioning process. Further, understanding the relationships between fly ash properties and fabric filter performance should lead to more reliable particulate control technologies that can ensure the lowest level of fine particle emissions at a reasonable cost. It is expected that superior fine particulate control can be achieved at a reduced cost compared to existing technologies, either by employing flue gas conditioning or by other design optimization.

The work consisted of the following:

1. Review of methods to measure the cohesive properties of bulk powders and selection of one or more methods to be developed for application to fly ashes.

2. Design and construction of a bench-scale reentrainment device to evaluate the reentrainment potential of fly ash and to measure the gas flow resistance of fly ash.

3. Tests with a Powder Characteristics Tester primarily to determine the aerated and packed porosities of fly ashes and their tendency to compact.

4. Tests with a Cohetester, which provides a direct measure of the tensile strength of fly ash as a function of compaction pressure or porosity.

5. Measurement of the dust cake resistance coefficient, K_2, for conditioned and baseline fly ashes.

6. Measurement of reentrainment or breakthrough behavior of conditioned and baseline ashes with the reentrainment device.

4.2.2 Review and Selection of Measurement Methods for Cohesive Properties

A brief review of available methods to measure cohesive properties of bulk powders was completed. Specific methods considered included the Southern Research Institute's measurement of the effective angle of internal friction (16) and two instruments manufactured by Hosokawa Micron International, Inc. EERC had some experience with the angle of internal friction measurement as a result of measurements done by the Southern Research Institute (SoRI) for the EERC under a previous project. The J.R. Johanson Co. of San Louis Obispo, California, has a service to measure the handling properties of bulk solids by several different methods, but does not have an instrument available for purchase. Both the SoRI and the J.R. Johanson methods have merit, but, since neither method was available as an off-the-shelf instrument, no attempt was made to employ them at EERC. Rather, commercially available methods were chosen.

A Powder Characteristics Tester, manufactured by Hosokawa Micron International, Inc., was purchased by EERC just prior to this project year.

Preliminary measurements in support of previous work indicated that this instrument would be useful in helping to characterize the cohesive properties of fly ash. The instrument is specifically designed for measuring the physical characteristics of fine bulk powders and is capable of seven different mechanical measurements. These include 1) angle of repose, 2) compressibility, 3) angle of spatula, 4) cohesiveness, 5) angle of fall, 6) dispersibility, and 7) angle of difference.

A second instrument, manufactured by Hosokawa Micron International, Inc., called a Cohetester was selected and purchased by EERC. This instrument provides a direct measurement of the tensile strength of a bulk powder sample. Selection of this instrument was based on previous successful tensile strength measurements of conditioned and baseline fly ash samples, performed by Hosokawa Micron International, Inc.

4.2.3 Cohetester Tensile Strength Measurements

A question exists as to appropriate methods to quantify the cohesive characteristics of a bulk powder such as fly ash. It should be recognized that more than one type of measurement may be required to describe and predict dust collectibility behavior. Direct measurement of the tensile strength of a bulk powder would appear to be a good approach, because bag cleanability is likely to be directly related to the tensile strength of the dust cake. The Cohetester measurement has the additional advantage in that tensile strength can be determined as a function of porosity. Therefore, if the porosity of the dust cake is known, the actual tensile strength of the dust cake can be inferred from Cohetester measurements. Tensile strength is also likely related to the pore-bridging ability of the dust and the susceptibility of the dust to reentrainment, because these characteristics should depend on the dust "stickiness." Tensile strength can be considered as a direct measure of dust stickiness.

A schematic of the Cohetester is shown in Figure 23. The Cohetester measures the horizontal tensile force of the powder bed formed in the split cell consisting of two semicircles. There is no contact and thus no friction between the cell components during the testing sequence. An ash sample is placed in a 5-cm diameter cell split into two halves. One half of the cell is stationary, and the other half is suspended such that the cell can be pulled apart with minimal force when no powder is in the cell. When the powder bed is pulled, it is extended in the same direction as the tensile force. The Cohetester measures this displacement of the bed as well as the tensile force simultaneously, and the fracture curve is plotted on an x-y recorder. An example of the fracture curves is shown in Figure 24.

The range in compaction forces with the Cohetester is dependent on the compaction weights used to compress the sample. The lowest compaction force is determined by the lightest compaction weight used, which was 320 grams corresponding to a compaction of 16 grams of force per square centimeter (g_f/cm^2). Some compaction is necessary so that the ash sample will fracture along a plane when pulled apart, which allows for a valid tensile strength measurement. The highest compaction force is determined by the structural integrity of the suspended cell and is limited to a compaction weight of 5000 grams or a compaction pressure of 255 g_f/cm^2. All samples were tested at approximately six different compaction pressures over the same range from 16 g_f/cm^2 to 255 g_f/cm^2. In terms of inches of water, this is equivalent to a

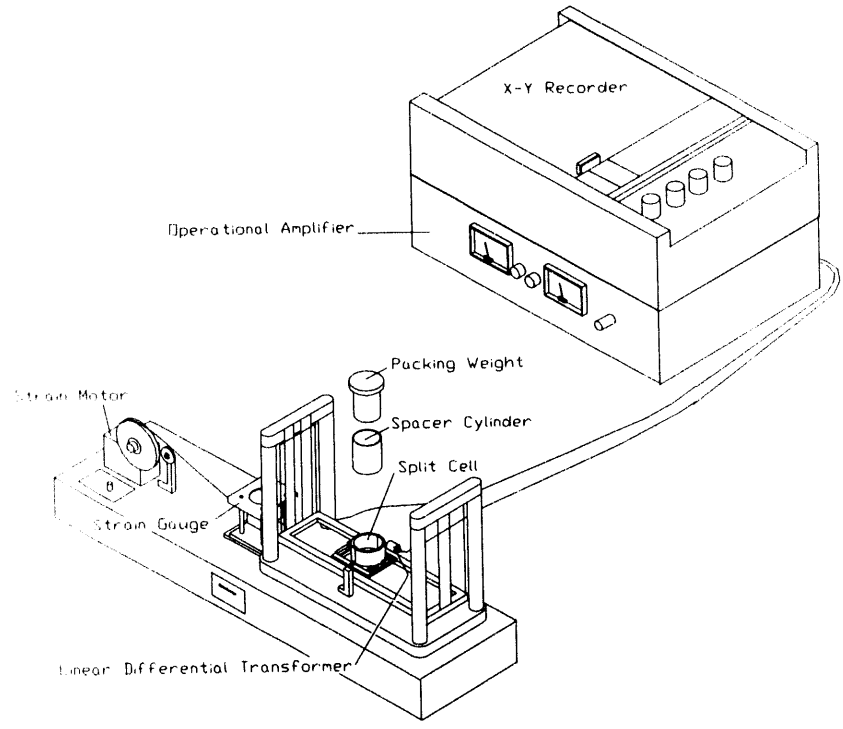

Figure 23. Schematic of the Cohetester.

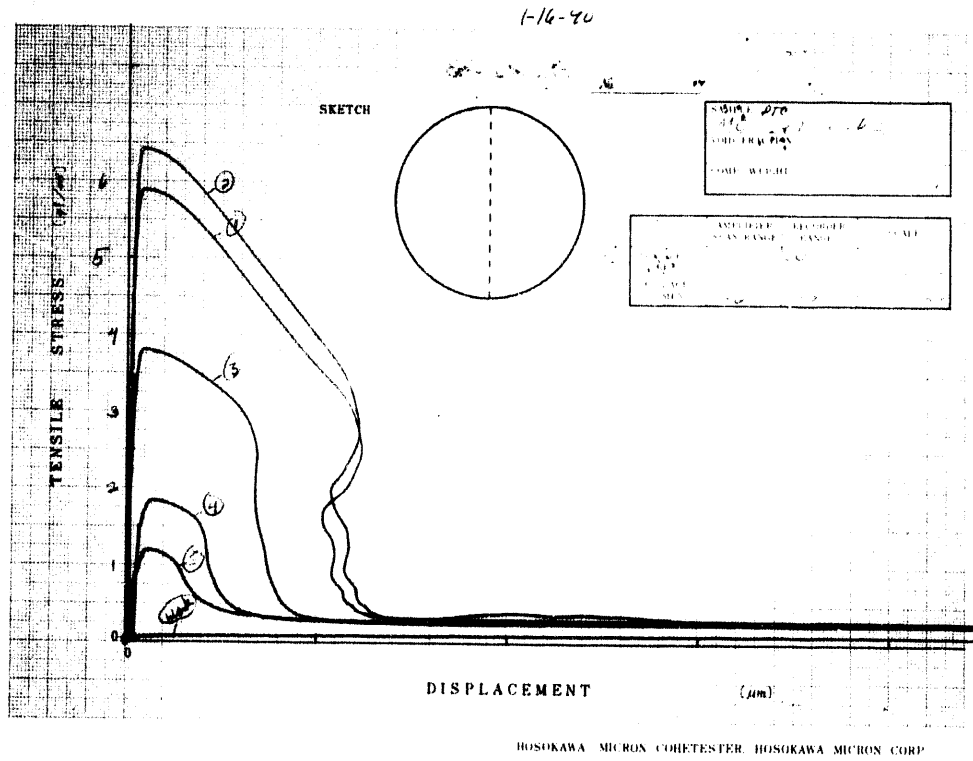

Figure 24. Example of fracture curves produced with the Cohetester, showing tensile strength as a function of displacement for several levels of compaction.

range from 6.3 to 100 inches of water. At the lowest compaction force, the pressure of 6.3 inches of water is a typical operating pressure drop for a fabric filter. An external compaction force, however, does not duplicate the pressure forces in a dust cake. With an ash sample compressed by an externally applied force, such as a compression weight in the Cohetester, the entire sample is subjected to the same approximate compaction pressure (ignoring the weight of the ash sample). For a dust cake in an operating baghouse, there is a pressure gradient across the thickness of the cake, and the compression force at the surface of cake is minimal compared to the compression force at the bottom (downstream surface). Therefore, the actual porosity in a dust cake is likely to be lower at the bottom of the cake where the compaction pressure is greater compared to the top surface of the cake. Such differences in porosity may be the result of sudden cake collapse that sometimes occurs as the pressure drop increases. While the Cohetester may not be able to duplicate the exact porosity conditions in a dust cake, tests at the lowest compaction pressure (16 g_f/cm^2) are probably the most indicative of dust cake conditions. Multiple tests at different compaction forces provide information to plot cohesive tensile strength as a function of porosity for a given ash.

Cohetester measurements were completed on previously collected fly ash samples, including those from tests in which ammonia and SO_3 were used as conditioning agents upstream of a baghouse and from tests without conditioning (15). Analysis of samples with the Cohetester should help to provide a better understanding of and explanation for the reduced particulate emissions and baghouse pressure drop that occur with conditioning. Three composite samples of baghouse hopper ash were previously collected during each 500-hour baseline and conditioning test with Monticello coal (one composite sample per week). Initial Cohetester results with these 6 samples are shown in Figure 25. From these results we can conclude that conditioning significantly increased the cohesive tensile strength for a given porosity. The range in porosities was determined by the range in compaction force, which was the same for both conditioning and baseline tests. The maximum compaction force allowable with the Cohetester (255 g_f/cm^2) resulted in a porosity of 39% for the baseline samples and 53% for the conditioned samples. Similarly, the minimum compaction force (16 g_f/cm^2) resulted in a porosity of only 51% for the baseline samples, compared to 67% for the conditioned samples. These results show that another effect of conditioning is to greatly reduce the packing tendency of the ash.

Cohetester results for conditioned and baseline ash samples, collected during 100-hour tests with Pittsburgh No. 8 coal, are shown in Figure 26. Again, the conditioned sample had a much greater tensile strength at the same porosity, and the baseline sample had a much greater tendency to pack. While the difference between conditioned and baseline samples is obvious, there is also a difference comparing the cohesive curves with the Monticello samples in that, at the maximum compaction force, the tensile strength for the PittsburghNo. 8 samples is much lower. This comparison is more easily seen in Figure 27, where both sets of data are shown in addition to Cohetester results with a Beulah fly ash. An exponential curve is fit to each data set in Figure 27. In the limit of porosity approaching 100%, the tensile strength should approach zero. Interestingly, the conditioned Monticello and the Pittsburgh No. 8 data form the same approximate exponential curve, indicating

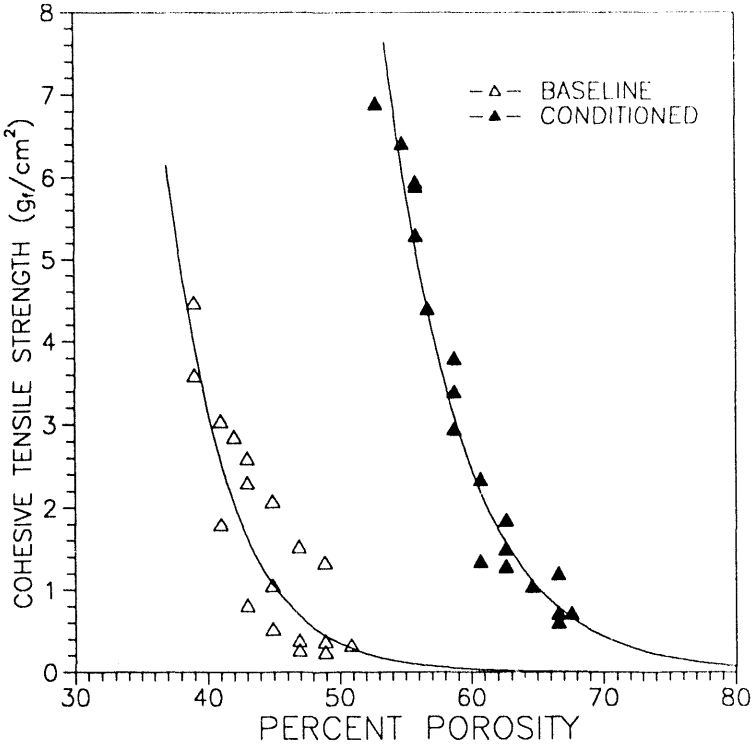

Figure 25. Cohesive tensile strength as a function of ash porosity for 500-hour Monticello ash samples as measured by the Cohetester method at approximately 30% relative humidity. Exponential curves are fit to each data set.

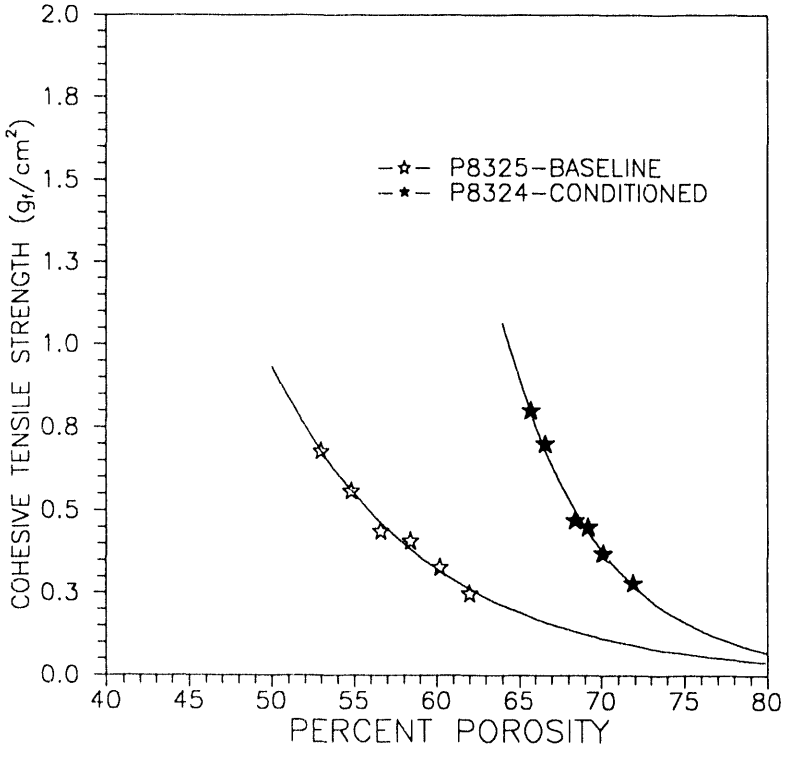

Figure 26. Cohesive tensile strength as a function of ash porosity for 100-hour Pittsburgh No. 8 ash samples as measured by the Cohetester method at approximately 30% relative humidity. Exponential curves are fit to each data set.

that, at the same porosity, they have the same tensile strength. However the compaction force required to attain the same porosity value is different--the Monticello sample having a greater tendency to compact. Previously measured particle-size distributions for the Monticello and Pittsburgh ashes did not indicate any significant differences in particle sizes. Therefore, the explanation for the differences in behavior between the Monticello and the Pittsburgh ashes is not clear. Possible additional influences include the amount of surface moisture on the ashes and the morphology of the particles. The Beulah ash sample (BU275) data closely follow the conditioned Monticello in terms of covering the same porosity range and forming the same approximate exponential curve as the conditioned samples. The Beulah ash had not been conditioned, but in previous work had shown excellent collectibility characteristics. No conditioning experiments have been done with the Beulah ash, but an interesting question is whether conditioned Beulah ash would form a tensile strength-porosity curve to the right of the baseline curve.

All of the Cohetester results shown in Figure 27 were completed in the winter when ambient laboratory relative humidity levels were typically about 30%. During the following summer, these measurements were repeated to determine the effect of elevated relative humidities on tensile strength. Ambient laboratory relative humidities ranged from 60% to over 80%. Cohetester measurements were performed at both the lower and higher humidity levels. Results with the same ashes at higher humidities are shown in Figures 28-33.

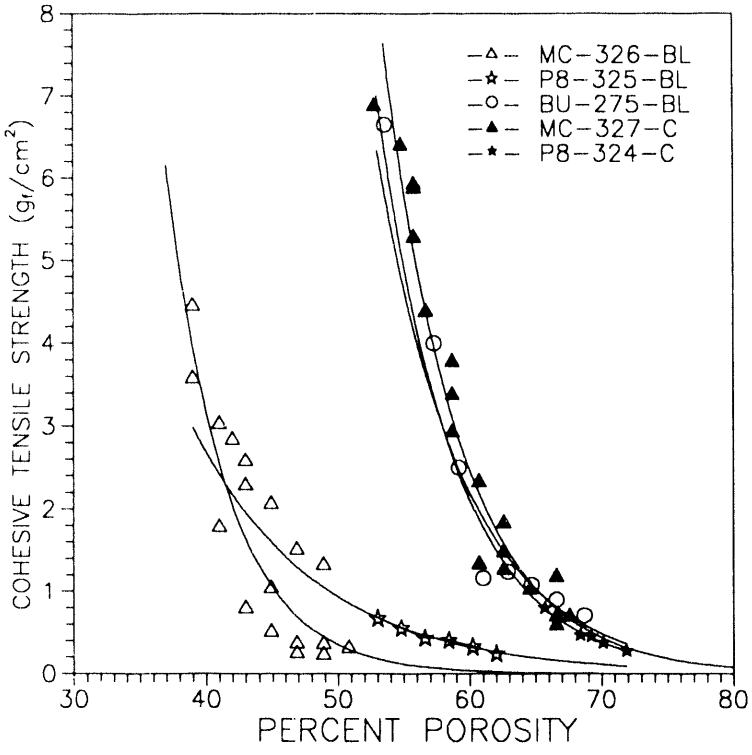

Figure 27. Cohesive tensile strength as a function of ash porosity for Pittsburgh No. 8, Monticello, and Beulah ash samples as measured by the Cohetester method at approximately 30% relative humidity. Exponential curves are fit to each data set.

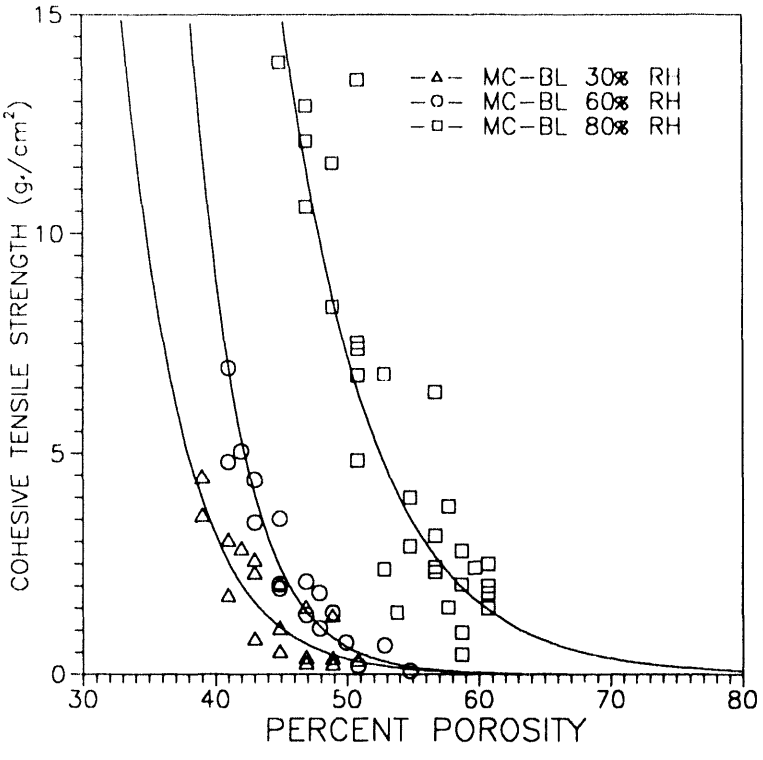

Figure 28. Effect of relative humidity on the cohesive tensile strength of 500-hour baseline Monticello fly ash. Exponential curves are fit to each data set.

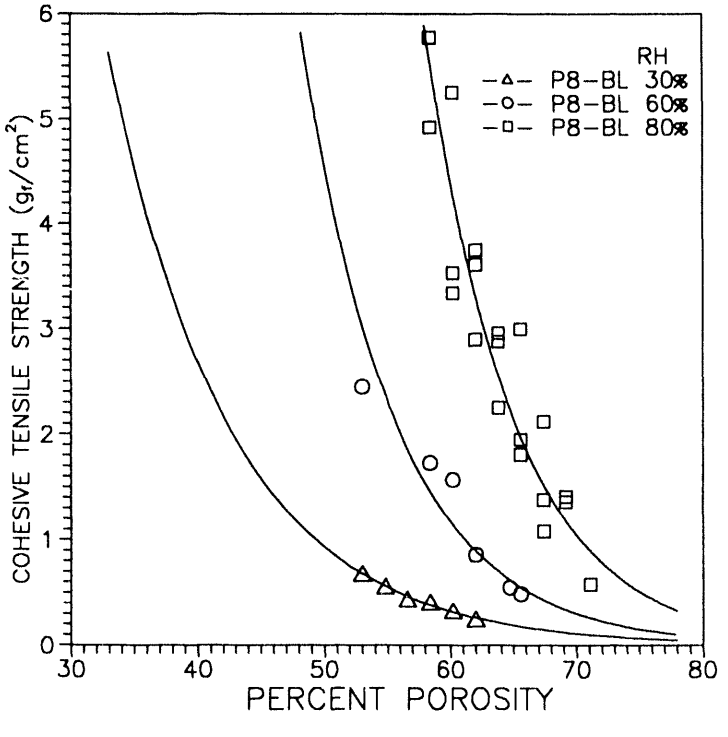

Figure 29. Effect of relative humidity on the cohesive tensile strength of 100-hour baseline Pittsburgh #8 fly ash. Exponential curves are fit to each data set.

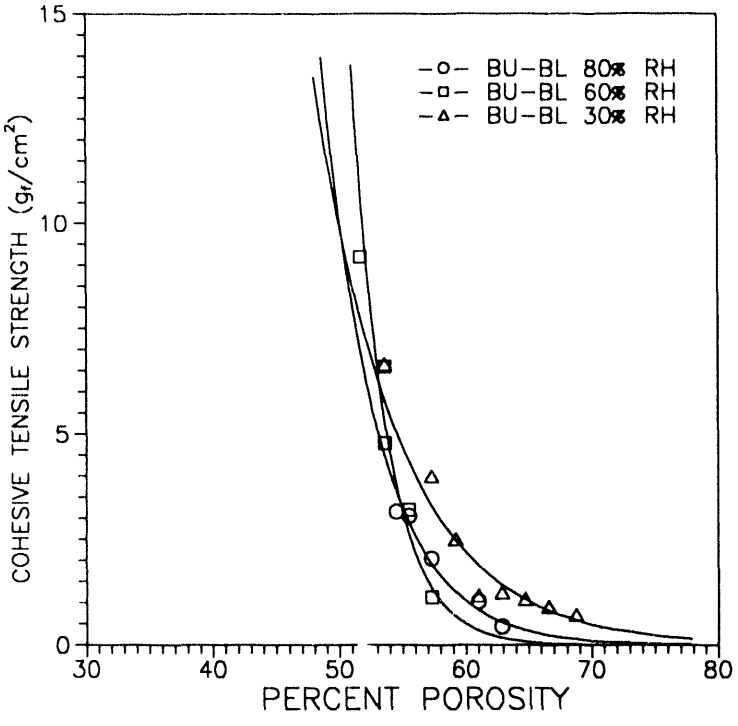

Figure 30. Effect of relative humidity on the cohesive tensile strength of Beulah fly ash. Exponential curves are fit to each data set.

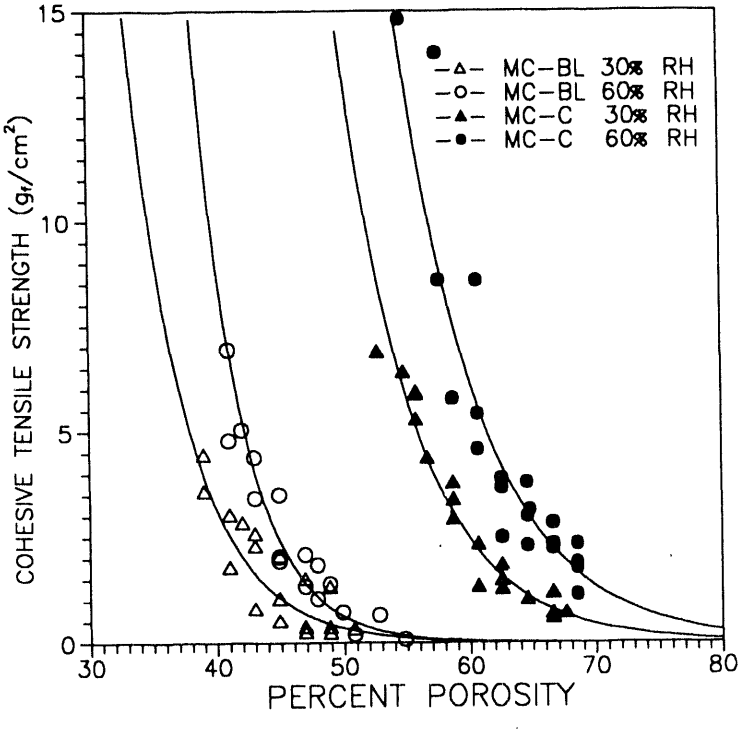

Figure 31. Comparison of shift in tensile strength curve as a result of increased relative humidity for 500-hour Monticello ash samples. Exponential curves are fit to each data set.

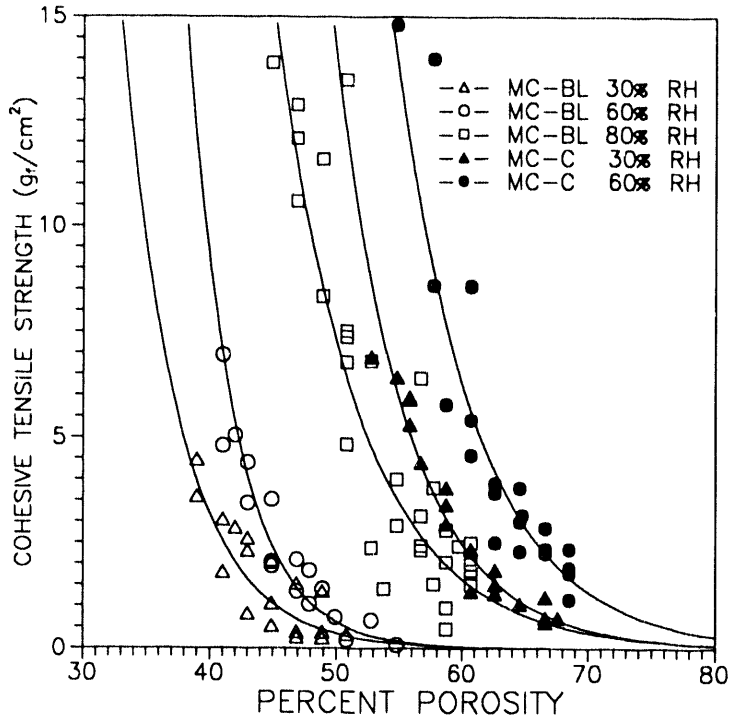

Figure 32. Comparison of shift in tensile strength curve as a result of increased relative humidity for 500-hour Monticello ash samples, including 80% relative humidity for the baseline ash. Exponential curves are fit to each data set.

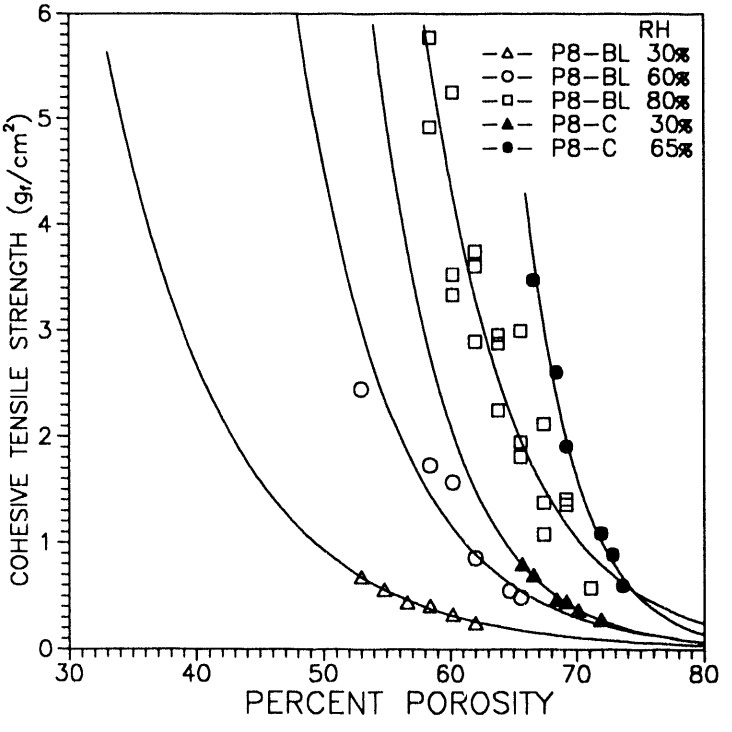

Figure 33. Comparison of shift in tensile strength curves as a result of increased relative humidity for 100-hour Pittsburgh #8 ash samples. Exponential curves are fit to each data set.

The effect of relative humidity on the baseline Monticello and Pittsburgh ashes, shown in Figures 28 and 29, is a shift of the tensile strength versus porosity curve to the right, similar to the effect of conditioning with ammonia and SO_3. From these data, the effect of relative humidity would appear clear, but relative humidity appeared to have little effect on the tensile strength of the Beulah ash, shown in Figure 30. A comparison between baseline and conditioned ashes with an increase in relative humidity from 30% to 60% is shown in Figure 31. In Figure 32, measurements of the baseline Monticello ash at approximately 80% relative humidity, added to the data from the previous figure, show that high humidity results in the same approximate tensile strength as conditioned ash at low relative humidity. In Figure 33, for the Pittsburgh #8 ash, the tensile strength curve for the highest humidity baseline ash is located to the right of the low humidity conditioned ash. Tensile strength measurements were not completed at 80% relative humidity for the conditioned Monticello and Pittsburgh #8 ashes because laboratory conditions did not remain at the high humidity level for a sufficient period. EERC plans to complete additional measurements during the next project year in which samples are stored for extended periods in a controlled humidity chamber, and Cohetester tests are also conducted within the chamber. From the Cohetester results over a wide range of relative humidities, we can conclude that relative humidity is an important parameter in the measurement of cohesive properties of fly ash.

A question exists as to whether the ambient relative humidity level is indicative of the effect of moisture on fly ash at 300°F in a baghouse. At temperatures above the boiling point, relative humidity may not be an appropriate term since the saturation level would be 100% moisture. However, in the loose interpretation of the term, if the flue gas moisture content were 10% at 300°F, this would correspond to only 10% relative humidity. Whether 10% relative humidity at laboratory conditions best simulates the effect of moisture at 300°F is unknown. At lower baghouse temperatures, such as downstream of a spray dryer where approach to saturation might be as low as 10°F, actual relative humidity may be as high as 80%. In this case, measurement of cohesive properties in the laboratory would likely give the best results, if completed at the same relative humidity. Another factor is the sensitivity of the individual ash to relative humidity. The cohesive properties of some ashes may be much more affected by small changes in relative humidity than other ashes. In spite of these questions, it appears that the Cohetester is an excellent method of measuring the tensile strength of fly ash. The tensile strength measurements clearly show the effect of conditioning on the ash and show that various ashes have their own distinct tensile strength curves. More work is needed to correlate these measurements with particulate emissions, but this method will likely be useful in helping to optimize the conditioning process.

4.2.4 Powder Characteristics Tester Results

A complete description of the powder characteristics tester and test methods were previously reported (15) and will not be repeated here. Of the seven measurements, the compressibility measurement appears to be the most useful. The compressibility measurement consists of determination of the aerated and packed density, which, along with particle density, provide

aerated and packed porosity. Compressibility is calculated from the aerated and packed densities by the equation:

$$C = 100\% \ (P - A)/P \qquad [1]$$

where compressibility is expressed as a percent, and P and A are the packed and aerated bulk densities. The aerated bulk density is obtained by sifting an ash sample through a vibrating 22-mesh screen into a 100-cc cup, so that dust overflows the cup edge. The excess dust is scraped off with a knife edge, and the weight of the known volume of dust is measured to determine the bulk density. The packed density is determined by adding an extension to the cup and filling the extension with additional sifted ash. The cup with the extension is then placed in a mechanism that raises the cup about 1/2 inch and lets the cup fall against a stop. This is done once per second for a period of 3 minutes. The cup extension is then removed, and the excess dust scraped off as before. There is no external compaction force on the dust layer. Compaction is caused by the natural settling that occurs as the dust is shocked. Results of these tests are shown in Table 6 for the baseline and conditioned samples. Three or four repeat tests were completed on each of the three baseline and conditioned baghouse ash samples from the 500-hour Monticello tests, and three repeat tests were completed on each of two samples from the 100-hour Pittsburgh #8 tests. Standard deviations shown in Table 6

TABLE 6

AERATED AND PACKED POROSITY[a]

Ash Type	Particle Density (g/cc)	Relative Humidity (%)	Aerated Porosity (%)	σ	n	Packed Porosity (%)	σ	n
Monticello baseline	2.53	30	62.6	0.6	9	40.1	0.8	9
Monticello conditioned	2.53	30	75.8	1.5	10	55.0	1.2	11
Monticello baseline	2.53	65	64.8	0.8	9	41.9	0.6	9
Monticello conditioned	2.53	65	81.3	1.0	9	60.3	1.0	9
Pittsburg #8 baseline	2.75	65	75.8	0.6	6	59.2	1.3	6
Pittsburg #8 conditioned	2.75	65	84.9	1.1	6	71.0	1.6	6

[a] Porosities are mean values for the given number of samples n, with standard deviation, σ.

include all baseline results grouped together and all conditioned results grouped together for each coal. Although there is slightly more data spread for the conditioned samples compared to the baseline samples, the effect of conditioning on the aerated and packed densities is very clear. These data demonstrate that the baseline ash has a high tendency to compact, and that conditioning imparts to the ash a resistance to packing. The results also show that relative humidity affects both the aerated and packed porosities for both baseline and conditioned Monticello samples. Measurements of the Pittsburgh #8 samples were not completed at the lower relative humidity, but further experimentation is planned during the next project year when these measurements will be completed inside a controlled humidity chamber.

It would appear that dust cake porosity might be predicted by correlating the aerated and packed porosities with actual dust cake porosity; however, not enough data are available. In addition, actual dust cake porosity may depend on other factors such as face velocity, fabric type, and cleaning method. Nevertheless, the aerated and packed porosity measurements would appear to be useful methods in helping to predict baghouse pressure drop. However, further experimentation is needed to determine the effect of relative humidity on the absolute values of both packed and aerated porosities.

4.2.5 Design and Construction of Reentrainment Cell

The intended function of the ash reentrainment test system was to study the reentrainment behavior of fly ash under flow conditions similar to conditions experienced in fabric filters. Schematics of the reentrainment cell and system, as initially designed, are shown in Figures 34 and 35. The intent was to measure the size and concentration of particles reentrained off the surface of a dust layer as a function of ash type, velocity, and porosity. The system was designed such that reentrained particles could be measured either with the carrier gas entering from the top or from the bottom of the dustcake. With the carrier gas flow entering the bottom of the dust layer, the dust layer is supported by a porous metal disk, and there is no support on top of the dust. With carrier gas flow downward, the dust is supported by screens or actual fabric. A second purpose of the device was to measure the pressure drop across a dust layer, again, as a function of dust type, gas velocity, and porosity. The study of these properties along with cohesive characteristics supports efforts to minimize fine particulate emissions from fabric filters.

4.2.6 K_2 Measurement and Analysis

K_2, the dust cake resistance coefficient derived from Darcy's law, was measured for each of the three composite baghouse hopper ash samples for the 500-hour baseline and conditioning tests with Monticello coal. To determine K_2, a 150-gram sample of ash was placed in the reentrainment cell, a cylinder with a porous bottom, and the pressure drop across the ash layer was measured at constant air flow rate through the dust for several levels of dust compaction. The porosity of the ash layer was calculated by measuring particle density by helium pycnometry and by measuring the dust layer thickness and cylinder diameter. Results of the K_2 measurements are shown in Figure 36, along with the Carman-Kozeny and Bush models that define K_2 in terms of porosity and particle size. The Carman-Kozeny relationship is derived from a

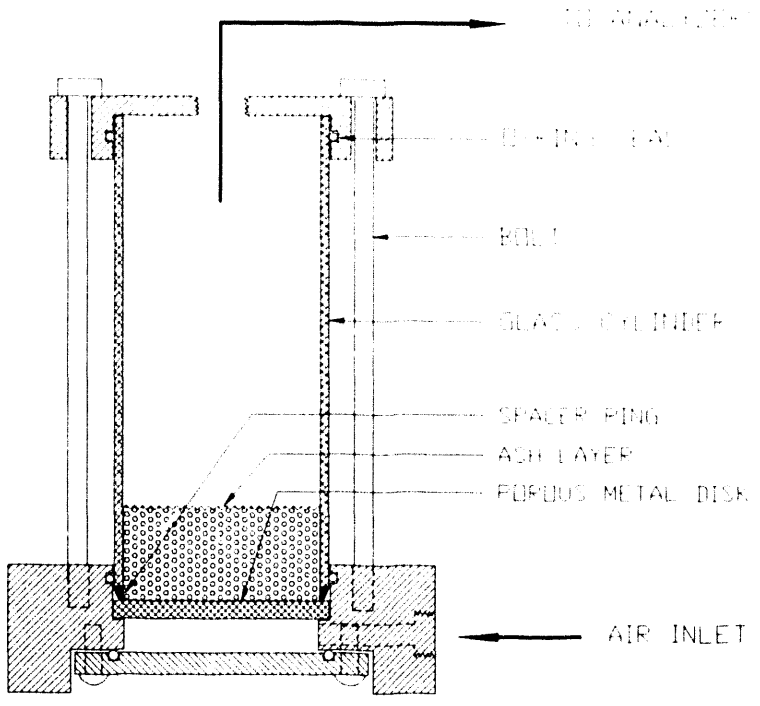

Figure 34. Fly ash reentrainment cell.

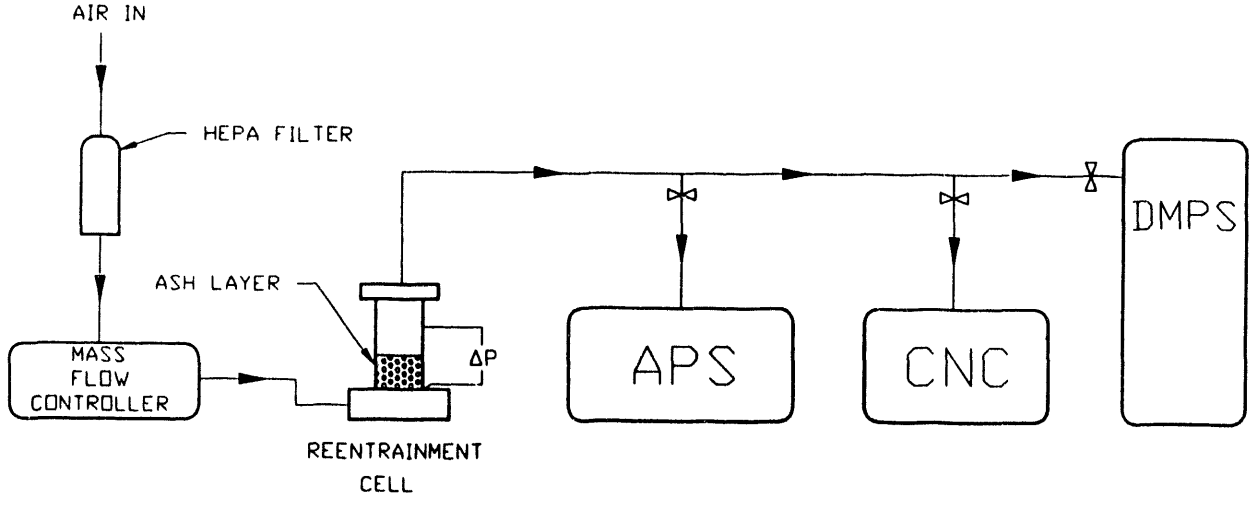

Figure 35. Fly ash reentrainment test system.

theoretical capillary model and, assuming spherical particles, takes the form (17):

$$K_2 = 36\ k\ \mu\ (1 - \epsilon)\ /\ \epsilon^3\ \rho_p\ D^2 \qquad [2]$$

where K_2 = specific dust cake resistance coefficient (sec/ft); note: K_2 can be converted to (in H_2O-ft-min)/lb by multiplying by a factor of 311.6.

k = Carman-Kozeny constant (~5) (dimensionless).

μ = gas viscosity (lb-sec/ft^2).
ϵ = porosity (dimensionless void volume fraction).
ρ_p = particle density (lb/ft^3).
D = particle diameter (ft).

Bush et al. and Cushing et al. (18,19) have reported an empirical relationship between K_2 and porosity for coal fly ash:

$$K_2 = (4\ \mu\ /\ D^2\ \rho_p)\ [(1 - \epsilon)/\epsilon]\ [7.5 + 9.1(1 - \epsilon) - 35.8(1 - \epsilon)^2 + 560(1 - \epsilon)^3] \quad [3]$$

where the D term is referred to as the drag equivalent diameter. In the Carman-Kozeny equation, D refers to the actual physical diameter for monosized spheres. For fly ash that has a broad particle-size distribution, the mass median diameter generally cannot be used for D for either equation. The value of the characteristic diameter is dependent on the particle-size distribution, specific surface area, and particle shape. These equations show that K_2 is most sensitive to particle size (or characteristic particle-size term) and porosity. Any attempt, then, to alter K_2 should focus on these properties, and any explanation of a change in K_2 must include particle size and porosity. A curve for each of the models was fit to the measured K_2 and porosity values for both the baseline and conditioned data (see Figure 36). It appears the

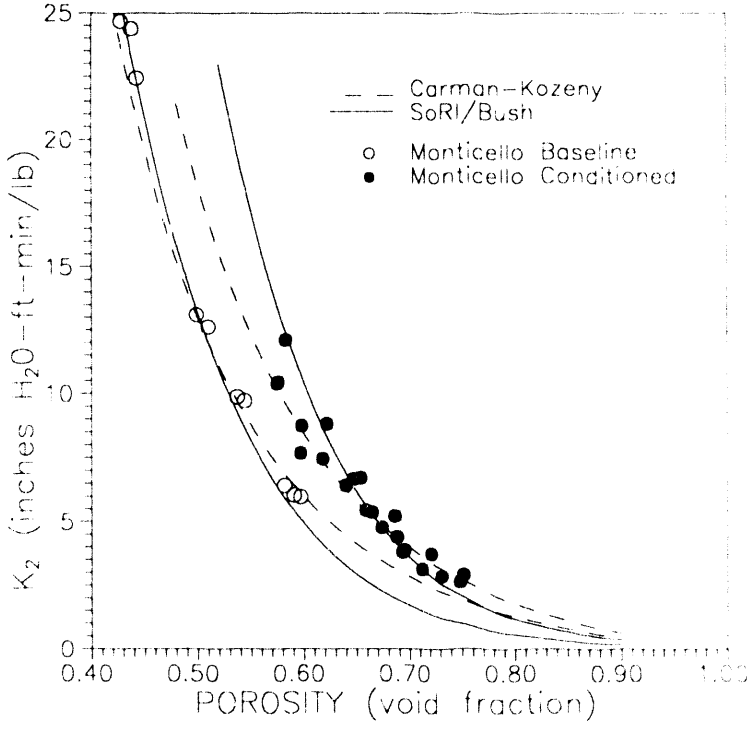

Figure 36. Specific dust cake resistance coefficient, K_2, as a function of ash porosity with Carman-Kozeny and SoRI/Bush models fit to data for 500-hour Monticello ash samples.

baseline data follow both models closely, while the data from the conditioned test seem to more closely fit the Carman-Kozeny relationship. Both the baseline and conditioned results represent data from three separate samples. For a single sample, the K_2 measurements should define a smooth curve with minimal data scatter, and such was the case for the individual samples. All data from the three baseline samples fit a smooth curve with little variability. While the three conditioned samples showed more variability, their composite data still define a distinct curve separate from the baseline data. The reason why the baseline and conditioned data formed separate curves is not clear. If the particle-size distributions and specific surface areas are unchanged, it is expected that the two data sets would define the same K_2 curve. Plausible explanations are that the particle-size distributions for the conditioned samples were somewhat smaller than the particle-size distributions for the baseline samples, or that the conditioned samples had an increased specific surface area. Previous data have not clearly indicated any shift in the fly ash particle-size distribution as a result of conditioning (11). Coulter counter data did show the volumetric median diameter of one of the conditioned samples to be 11 micrometers compared to 13 micrometers for the baseline samples, but extensive data were not taken, and specific surface area measurements have not yet been completed.

The explanation for why the porosity range was 43% to 60% (void fraction of 0.43 to 0.60) for the baseline data in Figure 36, while the conditioned data range was 58% to 75% is that the baseline ash had a much greater tendency to compact. Procedures were the same for all tests in that the same approximate compaction force was used to obtain the low porosity measurements, and no external compaction force was used to obtain the maximum porosity measurements. Ash porosity as a function of compaction force appears to be an important property of the dust which is also evident from other measurements.

Several important observations are obtained from the K_2 data and models in Figure 36. First, both the data and models demonstrate that a small increase in porosity can significantly reduce K_2. At constant dust cake weight and face velocity, this would correspond to a proportional decrease in baghouse pressure drop. Second, conditioning caused a distinct difference in the measured porosity range. These curves by themselves do not define the porosity of the baghouse dust cake, but it would appear to be a safe assumption that dust cake porosity for the baseline and conditioning tests would be somewhere between the respective minimum and maximum porosity values shown. The actual K_2 values of the dust cake during operation can be determined from dust loading and pressure drop data. The 500-hour tests were started with new bags, and the first 4 hours were conducted without bag cleaning. After the initial 4 hours, the tubesheet pressure drop was 10.5 inches of water for the baseline test and 2.15 inches of water for the conditioned test, which corresponds to a K_2 of 17 inches of water-ft-min/lb for the baseline test and 3.5 for the conditioned test. Looking at Figure 36, this implies that the dust cake porosity was about 47% for the baseline test and 71% for the conditioned test. K_2 can also be approximated by the increase in pressure drop between bag cleanings. From the previously reported (15) 500-hour tests, pressure drop increased about 6.5 inches (from about 3 to 9.5 inches) between the 2-hour bag cleaning intervals for the baseline test, compared to about 1.4 inches (from about 0.8 to 2.2 inches) for the conditioned test. These data result in somewhat higher K_2 values of 21 for the baseline test, corresponding to a dust cake porosity of 45% from Figure 36 and a K_2 of 4.5 for the conditioned test, corresponding to a dust cake porosity of 68% (from Figure 36).

From the bench-scale and baghouse K_2 data, we concluded that the actual dust cake porosity for the 500-hour baseline test was in the range of 45% to 47% and for the 500-hour conditioned test in the range of 68% to 71%. Looking at the tensile strength values for these porosity ranges (Figure 25) provides an interesting result. The corresponding tensile strength for the baseline tests is in the range of 0.7 to 1.0 g_f/cm^2 compared to 0.4 to 0.6 g_f/cm^2 for the conditioned tests. While there is some data scatter in this porosity range for the baseline tests, and extrapolation of the conditioned data was necessary to obtain the tensile strength value for the highest porosity, the results indicate that the actual tensile strength of the dust cake decreased with conditioning rather than increased. This result was not predictable, because previous measurements of ash pellet strength (6) and effective angle of internal friction (11) showed that conditioning causes an increase in the cohesive strength of the ash. However, this result is highly desirable because it would appear that bag cleanability would be directly related to the actual dust cake tensile strength. A reduction in dust cake tensile strength should facilitate bag cleaning. These results should be considered preliminary and need to be verified with other tests. The Cohetester tensile strength measurement, however, appears to be a good method to evaluate fly ash for fabric filter performance and possibly to predict bag cleanability.

To summarize the effect of conditioning on baghouse pressure drop, several measurements show a significant increase in ash porosity, which directly translates to increased dust cake porosity and reduced baghouse pressure drop. The lower pressure drop in turn reduces the compaction pressure on the dust layer, allowing a high porosity to be maintained. The reverse is true for the baseline ash or any ash that has a high tendency to compact. The tendency to compact causes high pressure drop, which results in a greater compaction force, leading to even lower porosity and higher pressure drop. Therefore, a treatment, such as ammonia and SO_3 conditioning, that reduces the compaction tendency of the ash can be effective in reducing baghouse pressure drop.

4.2.7 Reentrainment Tests

Initial tests were conducted with the reentrainment cell in which the ash was supported with a porous stainless steel disk on the bottom of the cell with gas flow upward. The intent was to measure particulate emissions with the aerodynamic particle sizer (APS) and the condensation nucleus counter (CNC) as the velocity was slowly increased. However, two phenomena made these initial tests largely unsuccessful. With an ash layer thickness greater than about two centimeters, the whole dust layer would lift as one continuous cake. The layer would begin lifting at a velocity that was much lower than typical filtration velocities and before any noticeable reentrainment was detected. Secondly, when a very thin dust layer was employed, small portions of the dust layer would lift prior to noticeable reentrainment. As soon as a portion of the dust layer would lift, the differential pressure across the layer would drop, and most of the gas flow would follow the path of least resistance, so there would be a section of high velocity. This made it impossible to measure the velocity at which reentrainment was detected. Mathematical analysis of this phenomenon revealed that this behavior is expected for fly ash with high K_2 values.

A dust cake will lift when the upward force (F_{up}) due to differential pressure (ΔP) is equivalent to the dust cake weight.

$$F_{up} = \Delta PA = F_{down} = WA \quad [4]$$

where "W" is the areal dust cake weight or weight per unit area (lb/ft^2).

The pressure drop across a dust cake is given as:

$$\Delta P = K_2 WV \quad [5]$$

where: ΔP = pressure drop (in H_2O).
K_2 = specific dust cake resistance coefficient (sec/ft); note K_2 can be converted to (in H_2O-ft-min)/lb by multiplying by a factor of 311.6.
W = areal dust cake weight (lb/ft^2).
V = face velocity (ft/min).

The condition when the dust cake will lift is:

$$\Delta PA = WA \quad [6]$$

substituting for ΔP:

$$K_2 WVA = WA \quad [7]$$

or

$$K_2 V = 1. \quad [8]$$

The term $K_2 V$ is dimensionless, if K_2 is given in terms of min/ft. In the case of K_2 given in terms of (in H_2O-ft-min)/lb, the relationship becomes:

$$5.19 K_2 V = 1 \quad [9]$$

Lifting velocity is:

$$V = 1 / 5.19 K_2 \quad [10]$$

where: V = face velocity (ft/min).
K_2 = specific dust cake resistance coefficient.

This means that for a low K_2 value of 1.0 inches of water-ft-min/lb, the velocity at which the cake will lift is only about 0.2 ft/min, a factor of 10 lower than a typical face velocity of 2 ft/min employed in a reverse-gas fabric filter.

Lifting velocity would appear to be the same as what is known as minimum fluidization velocity. Kunii and Levenspiel (20) give the minimum fluidization velocity for small particles (Reynolds number < 20) as:

$$V_{mf} = \frac{(\phi_s d_p)^2}{150} \quad \frac{\rho_s - \rho_g}{\mu} \quad g \left[\frac{\epsilon_{mf}^3}{1 - \epsilon_{mf}} \right] \qquad [11]$$

Where: V_{mf} = minimum fluidization velocity (cm/s).
ϕ_s = sphericity term for nonspherical particles (dimensionless).
d_p = particle size (cm).
ρ_s = solid or particle density (g/cm^3).
ρ_g = gas density (g/cm^3).
μ = gas viscosity (g/cm-s).
g = acceleration of gravity (980 cm/sec^2).
ϵ_{mf} = void volume fraction at minimum fluidization velocity (dimensionless).

This equation is similar to the Carman-Kozeny relationship given on page 42. In fact, setting the sphericity term at 1.0 and ignoring the gas density term, since $\rho_s >> \rho_g$, the two equations are almost identical. The acceleration of gravity term, g, is included in the viscosity term in Carman-Kozeny. Finally, the k constant in Carman-Kozeny is usually set at 5, but if k is set at 4.17, the Carman-Kozeny equation for K_2 is the inverse of the minimum fluidization velocity:

$$V_{mf} = 1 \; / \; K_2 \qquad [12]$$

This analysis shows that lifting velocity is the same as minimum fluidization velocity and is defined completely by $1 / K_2$. A question exists as to why the dust layer does not fluidize like bubbling fluidized beds with much larger particles. The answer is that, in the case of the whole cake lifting, the action does constitute fluidization in that one large bubble forms that is as large as the diameter of the cell. With a much larger diameter cell and a deep enough bed, the bubbles would form, and the ash would fall back to the bed as the bubbles break through the surface. However, the particles will not fluidize as individual particles, but as agglomerates. The size of the agglomerates would likely depend on the cohesive properties of the ash. Considering the case in which dust is supported by a woven fabric in which the pore size formed by the yarn junctions may be several hundred micrometers, the

face velocity is typically much greater than minimum fluidization velocity. Since typical median particle size may be only 10 micrometers, the potential exists to fluidize the dust that bridges over the large pores. If the dust did fluidize at the large pores, this would be a type of reentrainment because the fluidized dust would be carried to the clean side of the fabric. While the face velocity is usually much greater than the minimum fluidization velocity, large pores in woven fabrics can still be effectively bridged over. However, this means that the dust must have cohesive forces greater than the fluidization forces to maintain the pore bridges. Whether the dust can effectively bridge a given pore is likely to be a strong function of the face velocity, pore dimensions, and dust cohesive properties. It is well documented that if pores are not effectively bridged, pinholes can form in the dustcake (11,21). However, to our knowledge, prediction of pinhole formation in terms of face velocity, pore size, and dust properties has never been proposed.

To address this question, subsequent reentrainment tests were conducted in which the dust was supported by several screens, ranging from 50 mesh to 400 mesh, and by a woven glass fabric (601E type fabric used in previous conditioning work). The screen was placed in the bottom of the reentrainment cell in place of the porous disk. A layer of ash was then placed on the screen, and the gas flow was downward through the layer. Pressure drop and particulate emissions were measured as a function of velocity as the velocity was slowly increased. Additional variables included dust type (conditioned and baseline Monticello ash), sample weight (ranged from 2.6 to 49 grams), and porosity (altered by different levels of packing). Results showed that particulate emissions increased greatly when velocity was increased to an apparent critical breakthrough level. With the larger size screens, this was usually accompanied by a sudden decrease in pressure drop and obvious pinhole formation. Because the increase in emissions was large and instantaneous, the CNC was best suited to measure emissions, since it monitors in real time. An example of one of the tests with a 50-mesh screen and the conditioned Monticello ash is shown in Figure 37. Note that one large hole is obvious along with three smaller pinholes and some obvious cracks. The large hole was typical of results with the 50-mesh screen and was likely formed initially from smaller pinholes which grew in size as the local pinhole velocity increased. The cracks formed during many of the tests as the face velocity (and subsequent pressure drop) was increased. The formation of cracks is an indication of dust cake compression as the compaction force of the differential pressure was increased. Many times during testing, cracks formed prior to the detection of noticeable particulate penetration and prior to pinhole formation.

Results of all the reentrainment tests are shown in Table 7. The velocity and pressure drop are values at which major breakthrough of particulate emissions occurred, as measured by the CNC. K_2 is calculated from the velocity, pressure drop, and weight of the dust cake. When cracks are present, the K_2 values may not represent the actual K_2 of the continuous dust cake, but will be lower because of some gas flow through the cracks. The tests in Table 7, numbered 1 through 36, represent distinct ash samples, while subtests labeled a,b,c, etc., represent additional tests with the same ash sample in which the pinholes were bridged over after initial breakthrough by shocking the dust layer. Therefore, the "b" tests were usually packed more than "a" tests and had a higher K_2, and "c" tests had an even higher K_2 than the "b" tests.

Perhaps the most important result is the velocity at which breakthrough occurs for a given pore size, because this may be an indication of the maximum face velocity that can be employed. The velocities at which breakthrough occurred are shown as a function of screen type in Figure 38. All of the data for each screen size and dust are shown as a mean value along with the standard deviation. The breakthrough velocities for the conditioned ash increase with smaller pore sizes, as would be expected, and the breakthrough velocity for the 601E fabric was between the 150-mesh and 270-mesh screens. For the baseline ash, the breakthrough velocities were considerably lower than corresponding velocities with the same screen with the conditioned ash. Average breakthrough velocity for the 400-mesh screen was lower than the value for the 270-mesh screen. This can be explained in that the tests with the 270-mesh screen were conducted at higher K_2 values (see Table 7). At the highest K_2, breakthrough velocity tended to be higher. Therefore, perhaps a better evaluation of the results in Table 7 would be to combine breakthrough velocity and K_2 into one term. High breakthrough velocity and low K_2 are desired to achieve the lowest particulate emissions and lowest pressure drop, so the ratio of velocity to K_2 may be a better "performance index," as shown in Figure 39. Here, each dust type follows a more well-defined curve, with small standard deviations in most cases. Note that the velocity to K_2 index for the 601E fabric falls between the 150-mesh and 270-mesh screens.

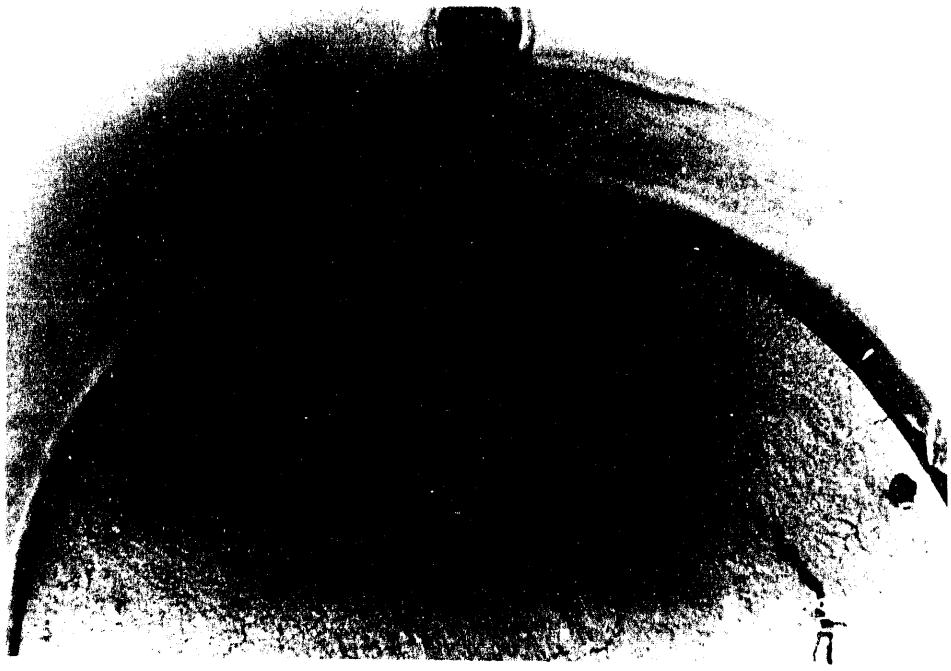

Figure 37. Example of breakthrough of ash with reentrainment cell. Conditioned 500-hour Monticello ash was supported with a 50-mesh screen.

TABLE 7

ASH REENTRAINMENT TESTS

Test	Ash	Screen (mesh)	Sample Wt (g)	Gas Flow (scfh)	Velocity (ft/min)	ΔP (in H_2O)	K_2*	V/K_2**
1	MC-C	50	32.0	3.00	1.7	5.9	1.5	1.09
2a	MC-C	50	25.5	1.80	1.0	2.3	1.2	0.80
2b	MC-C	50	25.5	2.50	1.4	5.0	1.9	0.71
2c	MC-C	50	25.5	2.30	1.3	6.0	2.5	0.50
3a	MC-C	50	24.0	3.40	1.9	7.5	2.3	0.83
3b	MC-C	50	24.0	3.50	1.9	11.6	3.4	0.57
3c	MC-C	50	24.0	5.50	3.0	21.4	5.0	0.76
4a	MC-C	50	24.3	3.80	2.1	7.9	2.1	0.99
4b	MC-C	50	24.3	3.20	1.8	10.7	3.4	0.52
14	MC-C	150	9.3	17.00	9.4	20.0	3.1	3.01
15	MC-C	150	9.1	8.00	4.4	7.7	2.6	1.69
16	MC-C	150	6.1	10.00	5.5	6.2	2.5	2.20
17	MC-C	150	26.1	6.00	3.3	11.3	1.8	1.86
18	MC-C	150	2.6	3.00	1.7	0.3	1.0	1.64
19	MC-C	150	8.5	11.00	6.1	8.9	2.4	2.59
25	MC-C	270	7.6	12.00	6.6	3.6	1.0	6.81
26	MC-C	270	7.1	12.00	6.6	3.0	0.9	7.63
27	MC-C	400	9.7	26.30	14.5	7.0	0.7	21.46
28	MC-C	400	9.1	24.50	13.6	20.0	2.2	6.11
35	MC-C	601E (fabric)	4.7	8.00	4.4	2.3	1.5	2.93
36	MC-C	601E (fabric)	12.0	12.00	6.6	17.5	3.0	2.21
5a	MC-BL	50	2.1	0.75	0.4	3.0	3.9	0.11
5b	MC-BL	50	25.1	0.90	0.5	5.7	6.2	0.08
6a	MC-BL	50	49.2	0.70	0.4	6.9	4.9	0.08
6b	MC-BL	50	49.2	0.65	0.4	8.6	6.6	0.05
6c	MC-BL	50	49.2	0.50	0.3	8.0	8.0	0.03
6d	MC-BL	50	49.2	0.45	0.2	6.8	7.6	0.03
6e	MC-BL	50	49.2	1.10	0.6	24.4	11.1	0.05
7	MC-BL	150	24.9	3.50	1.9	17.7	5.0	0.39
8a	MC-BL	150	8.2	0.50	0.3	0.3	1.8	0.15
8b	MC-BL	150	8.2	0.50	0.3	0.5	3.0	0.09
8c	MC-BL	150	8.2	3.70	2.0	6.4	5.2	0.39
9	MC-BL	150	9.3	1.50	0.8	1.4	2.5	0.33
10	MC-BL	150	7.9	3.00	1.7	2.5	2.6	0.64
11	MC-BL	150	10.4	2.50	1.4	3.8	3.6	0.38
12	MC-BL	150	19.0	3.00	1.7	10.3	4.5	0.37
12-2a	MC-BL	150	39.2	2.30	1.3	20.7	5.7	0.22
12-2b	MC-BL	150	39.2	5.00	2.8	83.0	10.5	0.26
13a	MC-BL	150	10.9	1.90	1.1	3.6	4.3	0.24
13b	MC-BL	150	10.9	5.50	3.0	20.1	8.3	0.37
20	MC-BL	150	10.6	1.80	1.0	3.9	5.1	0.20
21	MC-BL	270	10.0	12.00	6.6	36.6	7.5	0.88
22	MC-BL	270	13.6	10.00	5.5	52.7	9.6	0.58
23	MC-BL	270	6.4	8.00	4.4	14.3	6.9	0.64
24	MC-BL	270	21.5	10.00	5.5	96.0	11.0	0.50
29	MC-BL	400	14.0	4.00	2.2	9.4	4.1	0.53
30	MC-BL	400	5.0	8.00	4.4	4.6	2.8	1.56
31	MC-BL	400	10.1	5.00	2.8	15.0	7.3	0.38
32	MC-BL	400	7.9	12.00	6.6	32.0	8.3	0.80
33	MC-BL	601E (fabric)	11.5	8.00	4.4	30.5	8.2	0.54
34	MC-BL	601E (fabric)	5.3	3.00	1.7	1.7	2.6	0.63

* Units of K_2 are--(in H_2O-ft-min)/lb.

** Units of V/K_2 are--lb/(in H_2O-min^2).

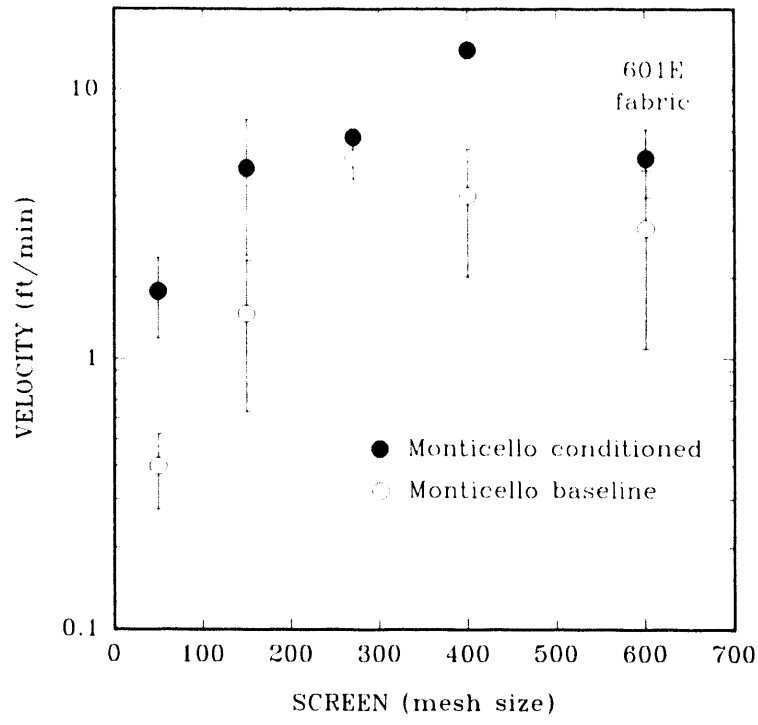

Figure 38. Velocity at which breakthrough penetration occurred as a function of screen type for 500-hour Monticello ash samples.

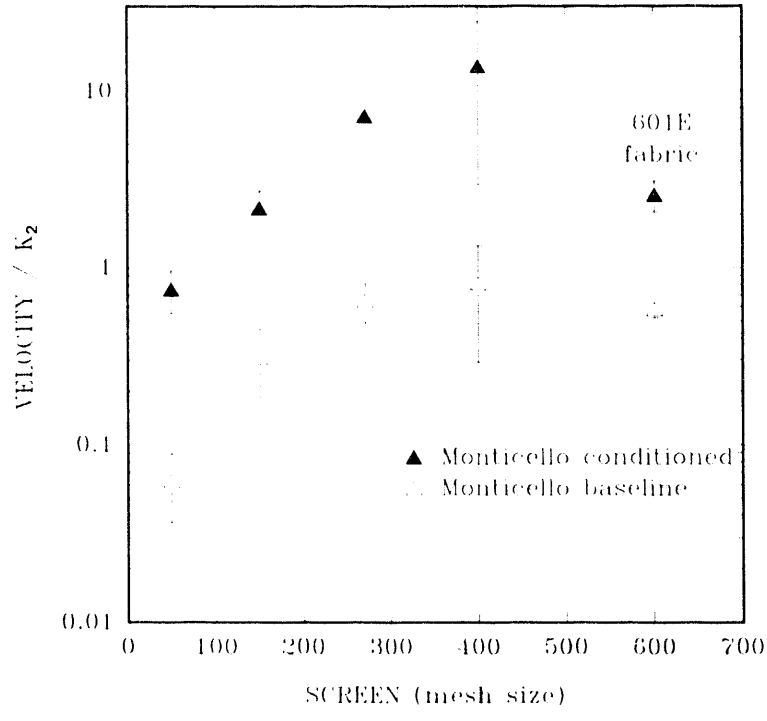

Figure 39. Ratio of velocity to K_2 at the point of breakthrough penetration as a function of screen type for 500-hour Monticello ash samples.

These tests were exploratory and need further refinement to be used as a method of predicting particle breakthrough. Since Cohetester measurements show that relative humidity can significantly affect tensile strength, further reentrainment tests should be conducted under carefully controlled humidity levels. The goal is not only to predict particulate emissions as a function of dust properties, but to optimize fabric filtration to achieve the lowest particulate emissions and pressure drop economically. The use of bench-scale tests to directly measure reentrainment behavior is one small step in achieving that goal.

5.0 CONCLUSIONS

Based on the results of work completed during the period July 1, 1989, through June 30, 1990, on the Flue Gas Cleanup Project, sponsored by the U.S. Department of Energy under the Cooperative Agreement (Contract No. DE-FC21-86MC10637), several conclusions are presented.

5.1 Catalytic Fabric Filtration

There was a substantial decrease in catalyst-coated fabric performance with increasing air-to-cloth ratio for all the fabrics tested. It appears that for the fabric samples tested, the maximum air-to-cloth ratio at which 85%-90% NO_x removal can be achieved is 3 ft/min. Although there was some variability in the data, the NO_x removal efficiency appeared to be constant with time for the short-term (8 hours) tests completed.

Fabric #2 (7 coats of 0.2 M 25% V + 75% Ti, no refractory undercoat, and a texturized weave) appeared to provide the best performance with respect to high NO_x removal efficiency and low ammonia slip. Fabric #13 (1 coat of 1 M 25% V + 75% Ti, 50% Si + 50% Ti undercoat, and texturized weave) also provided good performance and should be considered for use during future development activities. In addition, Fabrics #7 and #15 also will be considered for future work.

Although three of the coals, the two bituminous coals and the subbituminous coal, did not appear to affect the performance of the catalyst-coated fabric samples, the South Hallsville, Texas, lignite did result in lower NO_x removal and higher ammonia slip. This was probably caused by pinholes that formed in the dust cake, resulting in flue gas channeling through the fabric.

When the catalyst-coated fabric is exposed to flue gas, there is a decrease in both the quantity of catalyst on the fabric and in the total surface area. However, the percentage decrease in surface area is greater, indicating that a high percentage of the total surface area is located at or near the surface of the catalyst coating. A minimum surface area of 4.5 to 5 m^2/g and a vanadium concentration of 6 to 7 mg vanadium per gram of fabric appears to be necessary to achieve good catalyst-coated fabric performance.

5.2 Fine Particulate Control

Tensile strength measurements completed to date with the Cohetester show that this is an excellent method to quantify the cohesive character of fly ash. Furthermore, tensile strength measurements provide a partial explanation for the changes that occur in fly ash properties when flue gas conditioning is employed. This method should prove to be useful in not only optimizing the

conditioning process, but also in helping to model fabric filtration performance on the basis of dust properties. Tests at several relative humidities show that elevated humidity increases the tensile strength at constant porosity for some fly ashes, but the increase, if any, is ash specific.

Aerated and bulk porosity measurements also appear to be excellent methods of characterizing fly ash for the prediction of filtration performance. These measurements may lead to the prediction of actual dust cake porosity when more data become available. They are also useful in quantifying the changes in ash properties that occur with conditioning. Again, the effect of relative humidity needs to be considered when interpreting porosity measurements.

Reentrainment behavior of fly ash is more elusive to quantify. Experimental data and mathematical analysis show that the dust will lift or fluidize at a velocity defined by K_2^{-1}. This velocity is much smaller than typical filtration face velocities. Pore-bridging behavior can be quantified by the investigation of the breakthrough of dusts as a function of velocity and screen size; however, this method needs further refinement.

These three approaches to relating dust properties to filtration performance would appear to address the primary aspects of the filtration process. Tensile strength is likely related to dust cake release and may also be an indicator of particulate emissions. Porosity is directly related to baghouse pressure drop. Reentrainment tests provide a direct measure of pore-bridging behavior and should be a good predictor of particulate emissions. More work is needed, however, to further interpret data and combine results from all three methods into a single model.

6.0 RECOMMENDATIONS

Based on the results reported for Task B, Fabric Screening Tests, EERC believes that sufficient success has been achieved to warrant the initiation of pilot-scale development activities proposed for a non-Cooperative Agreement project. Funding for the pilot-scale development activities will be provided by the U.S. DOE and commercial interests.

Fifth year work under the Cooperative Agreement will involve limited bench-scale catalyst-coated fabric screening tests and will focus on bench-scale activities addressing fine particulate control. A maximum of two catalyst-coated fabric samples will be evaluated in conjunction with the setup and testing of a nitrous oxide (N_2O) analyzer. Measurement of N_2O concentrations will be made at the inlet and outlet of the fabric filter holder to verify that N_2O is not produced as a result of the NO_x reduction reactions occurring on the surface of the catalyst-coated fabric.

During the fifth year of the Cooperative Agreement more bench-scale work will be completed in an attempt to better correlate fly ash particle and dust cake characteristics to improvements in fabric filter performance as a result of flue gas conditioning.

7.0 REFERENCES

1. Weber, G.F.; Collings, M.E.; Schelkoph, G.L. "Simultaneous SO_x/NO_x Control," Final Technical Report for the Period April 1, 1987, through

March 31, 1988; Work performed under DOE Contract No. DE-FC21-86MC10637, Grand Forks, ND, May 1988.

2. Weber, G.F.; Collings, M.E.; Schelkoph, G.L.; Steadman, E.N. "Simultaneous SO_x/NO_x Control," Final Technical Report for the Period April 1, 1986 through March 31, 1987; Work performed under DOE Contract No. DE-FC21-86MC10637, DOE/FC/10637-2414, Grand Forks, ND, April 1987.

3. Weber, G.F.; Laudal, D.L. "SO_x/NO_x Control - Catalytic Fabric Filtration for Simultaneous NO_x and Particulate Control," Final Technical Report for the Period April 1, 1988 through June 30, 1989; Work performed under DOE Contract No. DE-FC21-86MC10637, Grand Forks, ND, August 1989.

4. Schonbucher, B. "Reduction of Nitrogen Oxides From Coal-Fired Power Plants by Using the SCR Process. Experiences in the Federal Republic of Germany With Pilot- and Commercial-Scale DeNox Plants," Presented at the 1989 EPRI/EPA Joint Symposium on Stationary Combustion NO_x Control, San Francisco, CA, March 1989.

5. Miller, S.J.; Laudal, D.L. "Real-Time Measurement of Respirable Particulate Emissions From a Fabric Filter," In Particulate and Multiphase Processes, Vol. 2. Contamination Analysis and Control; Ariman, T., Ed., Hemisphere Pub. Corp., 1987, p 663.

6. Miller, S.J.; Laudal, D.L. "Particulate Removal Enhancement of a Fabric Filter Using Flue Gas Conditioning," Presented at the Third EPRI Conference on Fabric Filter Technology for Coal-Fired Power Plants, Scottsdale, AZ, November 19-21, 1985.

7. Laudal, D.L.; Miller, S.J. "Flue Gas Conditioning for Improved Baghouse Performance," In Proceedings of the Sixth Symposium on the Transfer and Utilization of Particulate Control Technology; EPRI CS-4918, November 1986, Vol. 3, p 14-1.

8. Miller, S.J.; Laudal, D.L. "Flue Gas Conditioning for Improved Fine Particle Capture in Fabric Filters: Comparative Technical and Economic Assessment," In Low-Rank Coal Research Final Report, Vol. II, Advanced Research and Technology Development; DOE/FC/10637-2414, Vol. 2 (DE87006532), April 1987.

9. Miller, S.J.; Laudal, D.L. "Fine Particulate Emissions, Flue Gas Conditioning for Improved Fine Particle Capture in Fabric Filters," Final Technical Report for the Period April 1, 1987 through March 31, 1988; Work performed under DOE Contract No. DE-FC21-86MC10637, Grand Forks, ND, August 1988.

10. Laudal, D.L.; Miller, S.J. "Flue Gas Conditioning for Baghouse Performance Improvement With Low-Rank Coals," In Proceedings of the Fourteenth Biennial Lignite Symposium on the Technology and Utilization of Low-Rank Coals; University of North Dakota Energy and Environmental Research Center, Grand Forks, ND, 1987.

11. Miller, S.J.; Laudal, D.L.; Kim, S.S. "Mechanisms of Fabric Filter Performance Improvement With Flue Gas Conditioning," In Proceedings of the Seventh EPA/EPRI Symposium on the Transfer and Utilization of

Particulate Control Technology; EPRI GS-6208 Vol. 2, February 1989, pp 25-1.

12. Parfitt, G.D.; Sing, S.W. Characterization of Powder Surfaces; Academic Press: New York, NY, 1976.

13. Smith, D.L.O.; Lohnes, R.A. "Behavior of Bulk Solids," In Particle Characterization in Technology, Vol. I: Applications and Microanalysis; Beddow, J.K., Ed., CRC Press Inc.: Boca Raton, FL, 1984, p 101.

14. Cheney, J.L.; Homolya, J.B. "Sampling Parameters for Sulfate Measurement and Characterization," Environmental Science and Technology; Vol. 13, No. 5, May 1979, pp 584-588.

15. Miller, S.J. "Flue Gas Conditioning for Fabric Filter Performance Improvement," Final Project Report, Work performed under DOE Contract No. DE-AC22-88PC88866, Grand Forks, ND, December 1989.

16. Pohl, F.G. "A Novel Ring Shear Device for the Purpose of Classification of Fine Powders," Presented at the 17th Annual Meeting of the Fine Particle Society; San Francisco, CA, July 1986.

17. Sceidegger, A.E. The Physics of Flow Through A Porous Media; The Macmillian Co.: New York, NY, 1957.

18 Bush, P.V.; Snyder, T.R.; Smith, W.B. "Filtration Properties of Fly Ash from Fluidized-Bed Combustion," J. of the Air Pollution Control Assn. 1987, 37, 1292.

19. Cushing, K.M.; Bush, P.V.; Snyder, T.R. Fabric Filter Testing at the TVA Atmospheric Fluidized-Bed Combustion (AFBC) Pilot Plant; EPRI CS-5837, May 1988.

20. Kunii, D.; Levenspiel, O. Fluidization Engineering; Robert E. Krieger Pub. Co. Inc.: Malabar, FL, Reprint 1987.

21. Dennis, R., et al. Filtration Model for Coal Fly Ash With Glass Fabrics; EPA-600/7-77-084, August 1977.